Measurement of the Diffusion Coefficient of Miscible Fluids Using Moiré deflectometry

A Thesis

Submitted to the Graduate School
of Addis Ababa University
in Partial Fulfillment of the Requirements
for the Degree of
Master of Science in Physics

by

Sisay Milkias Waza

Graduate Studies, College of Natural of Science
Department of Physics
Addis Ababa, Ethiopia
February 2012

ADDIS ABABA UNIVERSITY
COLLEGE OF NATURAL SCIENCE
DEPARTMENT OF PHYSICS

Advisor : 22/3/12
Prof. A.V. Gholap

Examiners: .....
Dr. Tadelech Atomsa

.....
Dr. Abebe Belay

ABSTRACT

Measurements of the diffusion coefficient of two miscible liquids are reported. The liquids are various combinations of sodium chloride (NaCl) and pure water. The liquids were placed in a diffusion cell such that the interface is initially horizontal. As the fluids diffuse, the profile of the index of refraction near the interface is time dependent and is related to the local concentration of the diffusing fluids. The concentration gradient profile was measured, the experimental details and theoretical analysis for obtaining the magnitude of diffusion coefficient using the Moiré fringe patterns are described.

In this report the Moiré defelectometery method is applied for measuring the diffusion coefficient of NaCl in pure water at room temperature. The average diffusion coefficient was obtained by analysis of the measured concentration gradient profile, assuming that the diffusion process is one-dimensional and is characterized by a constant value of the diffusion coefficient (D). The value of $D = 1.58(\pm 0.05) \times 10^{-9}\ m^2/s$ is obtained for diffusion of NaCl molecules in pure water and it is in good agreement with the reported value in literatures.

ACKNOWLEDGEMENT

First of all I would like to thanks the Almighty God for giving me courage and support in order to accomplish the task of my Masters Thesis. God helps me a lot in all the stages of this thesis and gave me ideas to implement, things to achieve my desired goals.

I am truly indebted to Prof. A.V Gholap, my advisor, for his patience and guidance throughout my career in the past seven months. Likewise, I would like to thank Mr. Tewodros Abebe for providing me a Digital camera. I also want to thank Mr. Tesfaye Mamo who welcomed me in the lab warm heartedly and for his technical assistance.

I would specially like to thank to my mother Ms. Banchiyirga Hailemariam she is most important part of my life, for her efforts and courage she gave me. I would also like to thank my whole family my brothers Dergachew, Haileab and Geremew and my sister Mihret (Butu) for giving me moral support throughout the project.

TABLE OF CONTENTS

LIST OF FIGURES

LIST OF TABLES

CHAPTER - 1

1.1 Introduction

Diffusion is a process by which matter is transformed from one part of a system to another as a result of random molecular motion [1, 2]. Diffusion also describes the spread of particles through random motion from regions of higher concentration to regions of lower concentration [3, 4]. Diffusion can result from an external force field (forced diffusion) pressure gradients (pressure diffusion), temperature gradients (temperature diffusion, also called the Soret effect), and concentration gradients. The gradients of concentration plays an important role in many fields of chemistry and physics as well as in mechanical engineering and other fields such as crystal growth, pollution control, biological systems and separation of isotopes. The diffusion in the stationary liquid or gas phase is characterized by diffusion coefficient. The diffusion coefficient is the amount of a particular substance that diffuses across a unit area in one second under the influence of a gradient of one unit, and usually expressed in the units cm^2s^{-1}[5-7].

The diffusion coefficient of the miscible fluids is a property that is important in the dynamics. Its values are vitally important to the proper design of the reduced gravity experiments. In particular, it determines the desirable range for the speeds of the displacing fluids, so that the effect of diffusion is not overshadowed by convective transport of mass [8].

The diffusion coefficient of a substance in a fluid can be predicted theoretically or found from empirical correlations. It can also be obtained experimentally. Optical methods are among the wide variety of techniques available. They apply to transparent fluids and are based on the fact that the concentration distribution in a diffusion process produces a gradient in the index of refraction within the fluid. This gradient alters the optical pathlength of a light beam that traverses the medium, which causes it to exit the test section with a non-uniform phase and with spatially varying directions of propagation. By inverting data on the exit

phases and/or exit angles, the refractive index distribution is reconstructed. Together with a mathematical model of the diffusion process, the value of the diffusion coefficient is then obtained [9].

Diffusion in transparent liquids can be studied by various optical methods based on the measurement of refractive index variation, such as, for example, interferometry, holographic interferometry, sandwich holography, electronic speckle pattern interferometry(ESPI), speckle decorrelation, scanning laser beam, and common path interferometry [5]. Laser-based techniques are among the most sensitive methods employed for measuring diffusion coefficient and thermal conductivity. They have several distinct advantages over their direct contact counterparts, including the non-invasive nature of the measurement, remote monitoring and location of test/analysis equipment, imperviousness to harsh and corrosive environments, very high spatial precision, fast response times and high reliability and repeatability. Wave front comparison methods such as optical and holographic interferometry techniques are the most widely used techniques for diffusivity studies [6].

Those techniques that involve interference of wave fronts provide full-field refractive index data for the evaluation of concentration profiles. But the main limitation of the interferometric methods is their sensitivity to vibrations, and so they require precise optical conditions and limits their implementation in an industrial environment. Also, the acquired data has to be processed numerically to obtain derivative of the phase shift. This process may add to errors [5]. In this report the researcher use a high-precision, real-time, noninvasive, laser-based technique to measure the refractive index of a liquid mixture or an aqueous solution, which includes the Moiré deflectometry technique for direct mapping of ray deflection due to change in refractive index of a medium. Moiré deflectometry technique as presented by Kafri and Glatt [10] is a well-known method for mapping of ray deflections introduced by an object placed within a collimated laser beam.

Moiré deflectometry is a simple technique for optical testing of phase objects and specular surfaces, based on the moiré effect. The method provides mapping of ray deflections caused by either a phase object or reflection from a surface. From this information the index-of-refraction field of the phase object or the quality of the reflecting surface is obtained [11]. Moiré fringe patterns are formed by superimposing one of the Talbot (or Fourier) images of the first grating on the second one [12–14]. If an object is placed in front of first grating the light deflected by the object yields the shifted images, and the resultant Moiré fringes show the deflection mapping, depending on the distribution of the refractive index of the object. Moiré deflectometry is a simple and powerful tool for measuring ray deflections within the paraxial approximation. Measurements of deflection angles of 0.1° have been reported [15].

The main advantages of the Moiré deflectometry technique are its extreme experimental simplicity, low cost and low sensitivity to external disturbances in comparison with other interferometric methods that requires high prices and stable experimental set-up. The sensitivity of the Moiré deflectometry can be easily tuned to suit the requirement of an experiment by varying the gratings' pitch and their distance (where the diffraction effects are allowed). In a transparent mixture, change in concentration, for a multi-component liquid mixture, and temperature, results a change in the liquid index of refraction. A parallel laser beam, passing through such a medium of varying index of refraction, is locally deflected even if it passes perpendicularly to the gradient of the index of refraction (diffusion direction). The deflection angle is direct mapping of the refractive index gradient of the medium[5].

The Moiré Defelectrometry method is used by other researchers to find the diffusion coefficient of sugar solution, Kazem Jamshidi-Ghaleh and et al[6].
In this report Moiré deflectometry method is applied for measuring the diffusion coefficient of NaCl (salt solution) in pure water under 5-mW He–Ne laser (λ = 632.8 nm) illumination and its value is compared to the reported measurements

in the literature which are carried out using other methods such as Interferometric measurement [2], phase shifting interferometer [20].

1.2 General Objective

The general objective of the thesis is to determine the diffusion coefficient of NaCl in pure water using moiré deflectometry technique.

1.3 Specific objectives

The Specific objectives of the thesis are:

I, To determine the diffusion coefficient of different molar solution of NaCl in pure water using moiré deflectometry technique.

II, To compare the diffusion coefficient of different molar solution of NaCl in pure water.

CHAPTER – 2

2. DIFFUSION AND DIFFUSION COEFFICIENT

2.1. Diffusion

Diffusion is the physical process of matter spreading from a region of higher concentration to a region of lower concentration. Examples include the spreading of cream in a cup of coffee and the deflation of a helium balloon over time. In more general terms, diffusion may refer not only to the movement of matter but also of heat. For example, if one end of a block is heated rapidly and then the heat source is removed, over time the heat will diffuse through the block until the temperature of the block becomes uniform [17].

Diffusion can also be defined as the process where an initially nonuniform distribution of species in a mixture proceeds toward uniform distribution [5]. It is usually illustrated by the classical experiment in which a tall cylindrical vessel has its lower part filled with iodine solution, for example, and a column of clear water is poured on top, carefully and slowly, so that no convection currents are set up. At first the coloured part is separated from the clear by a sharp, well-defined boundary. Later it is found that the upper part becomes coloured, the colour getting fainter towards the top, while the lower part becomes correspondingly less intensely coloured. After sufficient time the whole solution appears uniformly coloured. There is evidently therefore a transfer of iodine molecules from the lower to the upper part of the vessel taking place in the absence of convection currents. The iodine is said to have diffused into the water [1, 2].

2.1.1 The theoretical basis of Diffusion

Atoms and molecules are constantly in motion. Each atom or molecule undergoes many collisions with others in the gas or liquid in a very short period of time. Because of this, the atom or molecule appears to move in a somewhat

random fashion, as illustrated in figure 1. This motion is often referred to as a random walk. [17]

If it were possible to watch individual molecules of iodine when it diffused into water, it would be found that the motion of each molecule is a random one. In a dilute solution each molecule of iodine behaves independently of the others, which it seldom meets, and each is constantly undergoing collision with solvent molecules, as a result of which collisions it moves sometimes towards a region of higher, sometimes of lower, concentration, having no preferred direction of motion towards one or the other. The motion of a single molecule can be described in terms of the familiar 'random walk' picture, and whilst it is possible to calculate the mean-square distance traveled in a given interval of time it is not possible to say in what direction a given molecule will move in that time.

This picture of random molecular motions, in which no molecule has a preferred direction of motion, has to be reconciled with the fact that a transfer of iodine molecules from the region of higher to that of lower concentration is nevertheless observed. Consider any horizontal section in the solution and two thin, equal, elements of volume one just below and one just above the section. Though it is not possible to say which way any particular iodine molecule will move in a given interval of time, it can be said that on the average a definite fraction of the molecules in the lower element of volume will cross the section from below, and the same fraction of molecules in the upper element will cross the section from above, in a given time. Thus, simply because there are more iodine molecules in the lower element than in the upper one, there is a net transfer from the lower to the upper side of the section as a result of random molecular motions [1].

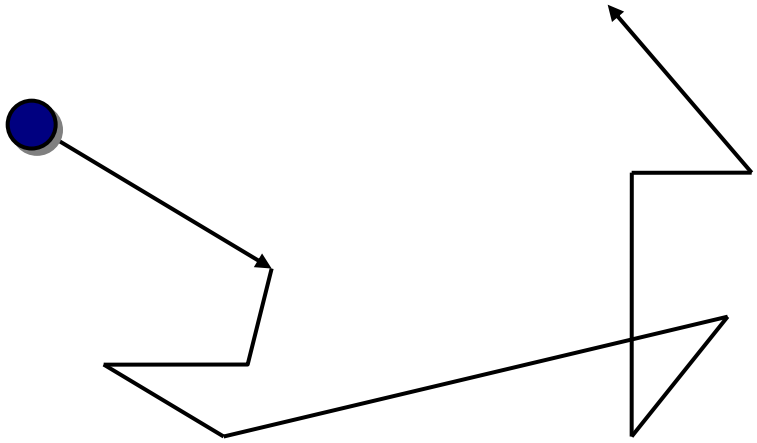

Figure 1 The motion of an atom or molecule in solution appears to be a random walk.

2.1.2 Basic hypothesis of mathematical theory of Diffusion

Fick's was the first to put diffusion on a quantitative basis by adopting the mathematical equation of heat conduction derived some years earlier by Fourier (1822). The mathematical theory of diffusion in isotropic substances is therefore based on the hypothesis that the rate of transfer of diffusing substance through unit area of a section is proportional to the concentration gradient measured normal to the section, i.e.

$$F = -D\frac{\partial C}{\partial x} \qquad \text{.....(1)}$$

Where F is the rate of transfer per unit area of section, C the concentration of diffusing substance, x the space coordinate measured normal to the section, and D is called the diffusion coefficient. In some cases, e.g. diffusion in dilute solutions, D can reasonably be taken as constant, while in others, e.g. diffusion in high polymers, it depends very markedly on concentration. If F, the amount of material diffusing, and C, the concentration, are both expressed in terms of the same unit of quantity, e.g. gram or gram molecules, then it is clear from equation (1) that D is independent of this unit and has dimensions $(\text{length})^2(\text{time})^{-1}$, e.g. $\text{cm}^2\ \text{s}^{-1}$. The negative sign in equation (1) arises because diffusion occurs in the direction opposite to that of increasing concentration.

It must be emphasized that the statement expressed mathematically by (1) is in general consistent only for an isotropic medium, whose structure and diffusion properties in the neighborhood of any point are the same relative to all directions. Because of this symmetry, the flow of diffusing substance at any point is along the normal to the surface of constant concentration through the point. In figure 2 it is clearly shown that in an anisotropic medium the diffusion properties depend on the direction in which they are measured [1].

2.1.3 Differential equation of diffusion

The fundamental differential equation of diffusion in an isotropic medium is derived from equation (1) as follows. Consider an element of volume in the form of a rectangular parallelepiped whose sides are parallel to the axes of coordinates and are of lengths $2dx$, $2dy$, $2dz$. Let the centre of the element be at $P(x, y, z)$, where the concentration of diffusing substance is C. Let $ABCD$ and $A'B'C'D'$ be the faces perpendicular to the axis of x as in figure 1. Then the rate at which diffusing substance enters the element through the face $ABCD$ in the plane $x - dx$ is given by:

$$4dydz\left(F_x - \frac{\partial F_x}{\partial x} dx \right) \qquad \text{.....(2)}$$

Where F_x is the rate of transfer through unit area of the corresponding plane through P. Similarly the rate of loss of diffusing substance through the face $A'B'C'D'$ is given by:

$$4dydz\left(F_x + \frac{\partial F_x}{\partial x} dx \right) \qquad \text{..... (3)}$$

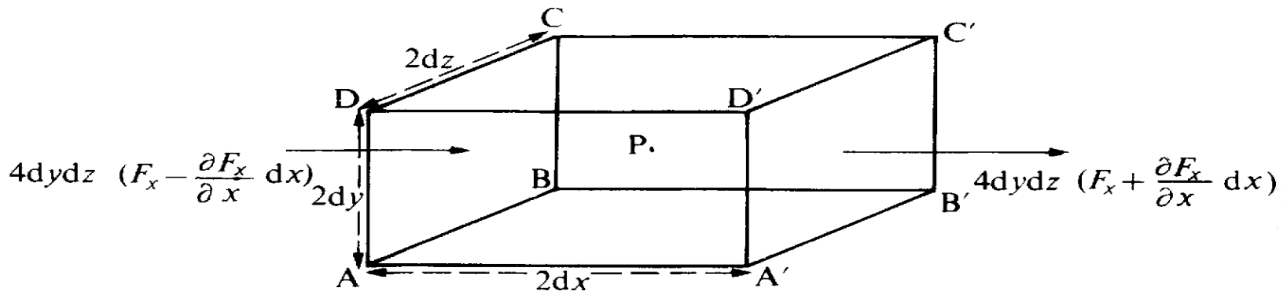

Figure 2 Element of Volume[1]

The contribution to the rate of increase of diffusing substance in the element from these two faces is thus equal to

$$-8dxdydz\frac{\partial F_x}{\partial x}$$

Similarly from the other faces we obtain

$$-8dxdydz\frac{\partial F_y}{\partial y} \qquad \text{and} \qquad -8dxdydz\frac{\partial Fz}{\partial z}$$

But the rate at which the amount of diffusing substance in the element increases is also given by

$$8dxdydz\frac{\partial C}{\partial t} \qquad \text{.....(4)}$$

and hence we have immediately

$$\frac{\partial C}{\partial t}+\frac{\partial F_x}{\partial x}+\frac{\partial F_y}{\partial y}+\frac{\partial F_z}{\partial z}=0 \qquad \text{.....(5)}$$

If the diffusion coefficient is constant, F_x, F_y, F_z are given by (1), and (5) becomes

$$\frac{\partial C}{\partial t} = D\left(\frac{\partial^2 C}{\partial x^2} + \frac{\partial^2 C}{\partial y^2} + \frac{\partial^2 C}{\partial z^2}\right) \quad \text{.....(6)}$$

and equation (6) reduced to

$$\frac{\partial C}{\partial t} = D\frac{\partial^2 C}{\partial x^2} \quad \text{.....(7)}$$

if diffusion is one-dimensional i.e. if there is a gradient of concentration only along the x-axis. Equations (1) and (7) are usually referred to as Fick's first and second laws of diffusion, since they were first formulated by Fick (1855) by direct analogy with the equations of heat conduction [1].

2.1.4 The Empirical laws of Diffusion

The phenomenological description of diffusion is embodied in Fick's two laws, which are empirical statements that relate the diffusive flow of matter to concentration gradients. To illustrate these laws, consider a single-phase dilute binary alloy in which the constituents are inhomogeneously distributed and let C be the concentration of the minor constituent. The concentration is function of position and time and the concentration gradient induces a flow of matter [2, 18].

2.1.4.1 Fick's First law

Fick's First law states that "the flux of the diffusing species in a given direction has a magnitude proportional to the concentration gradient in that direction". That is if J_1 the flux along the x_1 axis, then

$$J_1 = -D_1\frac{\partial C}{\partial x_1} \quad \text{.....(8)}$$

Where: D_1 is the proportionality factor called diffusion coefficient. The negative sign expresses the fact that diffusion occurs from the region of high concentration to region of law concentration [10].

If x_1, x_2, x_3 and i_1, i_2, i_3 are the points in a cartesian coordinate system and unit vectors respectively then we would expect that an equation similar to equation (8) hold for each of the three directions along the coordinate axis. For isotropic systems such as gases and liquids, this turns out to be the case. Further more for such systems the diffusing coefficient is experimentally found to be the same in all directions. In nonhomogeneous systems, however it is not the same in all directions. Also the flux in a one direction can depend on the flux in other directions [19].

These results can be described by a generalized Fick's first law, as follow

$$\left.\begin{aligned} J_1 &= D_{11}\frac{\partial C}{\partial x_1} - D_{12}\frac{\partial C}{\partial x_2} - D_{13}\frac{\partial C}{\partial x_3} \\ J_2 &= D_{21}\frac{\partial C}{\partial x_1} - D_{22}\frac{\partial C}{\partial x_2} - D_{23}\frac{\partial C}{\partial x_3} \\ J_3 &= D_{31}\frac{\partial C}{\partial x_1} - D_{32}\frac{\partial C}{\partial x_2} - D_{33}\frac{\partial C}{\partial x_3} \end{aligned}\right\} \quad \text{..... (9)}$$

Equations 9 can be written in a compact form by defining the vector J and the diffusion constant D as:

$$\left.\begin{aligned} J &= J_1 i_1 + j_2 i_2 + J_3 i_3 \\ D &= D_{11} i_1 i_1 + D_{12} i_1 i_2 + D_{13} i_1 i_3 + D_{21} i_2 i_1 + D_{22} i_2 i_2 + D_{23} i_2 i_3 + D_{31} i_3 i_1 + D_{32} i_3 i_2 + D_{33} i_3 i_3 \end{aligned}\right\} \text{...(10)}$$

Therefore the generalized Fick's first law can be written as:

$$J = -D\nabla C \quad \text{.....(11)}$$

2.1.4.2 Fick's Second law

Fick's Second law states that "the time rate of change of concentration in volume element of membrane with in the differential filed is proportional to the rate of change of flux gradient at that point in the filed" i.e.

$$\frac{\partial C}{\partial t} + \nabla \cdot J = 0 \text{.....(12)}$$

This is just an expression of law of conservation of matter and states that any change in concentration in a volume element is the result of the difference in matter flow in and out of the volume element [10,18]. Combining equations (11) and (12) gives a generalized form of Fick's second law:

$$\frac{\partial C}{\partial t} = \nabla D \cdot \nabla C \quad \text{..... (13)}$$

In isotropic and cubic systems this takes a particularly simple form since $D_1 = D_2 = D_3 = D$ [16, 20]. If D is a constant independent of position and time the simplification is even greater and Fick's second law becomes

$$\frac{\partial C}{\partial t} = \nabla^2 C \quad \text{..... (14)}$$

2.2 Diffusion Coefficient

The diffusion coefficient D has units of m^2s^{-1} and provides a measure of the number of molecules moving through a particular cross sectional area per unit of time. Experimental measurements of typical diffusion coefficients in water at 300K yield values in the range of 10^{-9} m^2s^{-1} [17].

2.2.1 Relation of Diffusion Coefficient to Mean Free Path

The average distance that an atom or molecule travels between collisions is called its mean free path. The mean free path depends upon the size of the atom or molecule. For a typical small molecule such as O_2 in the gas phase, the mean free path at 300K is about 80nm. Combining this with an average speed of 400m/s, on average the time between collisions for a small molecule is about $2\times10^{-10}s$, or $200PS$. Looking at this in another way, a typical small molecule undergoes about 5×10^9 collisions per second in the gas phase.

As a molecule undergoes this seemingly random motion, induced by collisions with other molecules, it migrates through the solution. If there was initially a larger proportion of molecules of a particular type in one region of the solution

(e.g., a drop of ink in a container of water), then over time the molecules will spread out and become evenly distributed throughout the solution: this is the process of diffusion. The diffusion of molecules throughout a solution is in accord with the second law of thermodynamics that states that the entropy change for a closed system must be positive (tending toward more randomness).

For an initial concentration gradient in a gas or liquid solution, the rate at which the molecules spread out is proportional to the difference in the concentration gradient (or curvature)[17].

Diffusion Rate = D × Concentration Curvature

Where D is diffusion coefficient gradient in $(\text{length})^2(\text{time})^{-1}$.

The diffusion coefficient is related to the mean free path that a molecule travels via the Einstein-Smoluchowski equation

$$D = \frac{\lambda^2}{2\tau} \quad \text{.....(15)}$$

In Equation (15), λ is the mean free path and τ is the average time between collisions. Assuming that the average time between collisions can be calculated from the average speed and the mean free path, the time between collisions can be expressed as

$$\tau = \frac{\lambda}{\nu_{ave}} \quad \text{.....(16)}$$

Where ν_{ave} is the average speed. Substituting this relation into the Einstein-Smoluchowski equation gives

$$D = \frac{1}{2}\lambda\nu_{ave} \quad \text{.....(17)}$$

Using the gas phase values of 80 nm for the mean free path and 400 m/s as the average speed, the predicted diffusion coefficient for a small molecule in the gas phase is much larger than the typical liquid phase diffusion coefficient. This is because, with fewer collisions in the gas phase, a molecule can move further

away from its starting point in a shorter period of time. The higher frequency of collisions in the liquid phase leads to slower diffusion [29].

2.2.2 Relation of Diffusion Coefficient to Viscosity

In the liquid phase, diffusion can be related to a measurable property known as viscosity. Viscosity is a measure of the resistance of a fluid to flow. A liquid such as water that flows easily has a relatively low viscosity, while a liquid such as syrup that is very thick and flows more slowly has a high viscosity. More specifically, the viscosity η of a liquid is a quantitative measure of the liquid's ability to transport momentum. The units of viscosity are Poise (P), typical viscosities are in the range of $10^{-4} P$ for gases and $10^{-2} P$ for liquids.

The relation between viscosity and the diffusion coefficient is given by the Einstein-Stokes equation,

$$D = \frac{KT}{6\pi r \eta} \quad \text{..... (18)}$$

Where K is the Boltzmann constant, T is temperature, and r is the radius of the molecule. Note that Equation (18) was derived assuming that the molecule was roughly spherical in shape. Qualitatively, the Einstein-Stokes equation shows that the viscosity and diffusion coefficient are inversely related. This makes sense when considering a molecule with a high viscosity flows slowly and thus would be expected to diffuse slowly [17].

2.2.3 The Statistical Model of Diffusion – Random Walks (one dimensional case)

Random numbers can be used in simulations of deterministic processes involving many (10^{23}) particles. Processes such as diffusion, in which a single particle moves through a solution containing a huge number of other particles, can be modeled. The other particles in the solution affect the dynamics of the particle of interest through interactions and collisions. Though in principle it would

be theoretically possible to write down the equations of motion for all the particles in the system, in practice this is not feasible. Therefore, the effects of the other particles in the solution upon the particle of interest can be modeled by assuming random motion.

The simplest example of this type of modeling is called a one-dimensional random walk. In this simulation, a random number between 0 and 1 is selected for each step. If the random number selected is less than 1/2, the walker takes a step of –1. If the random number selected is greater than or equal to 1/2, the walker takes a step of +1. The distance of the walker from the origin is monitored.

Two simulations illustrating the one-dimensional random walk are shown in figure 3. Each simulation was carried out for 1000 steps[21].

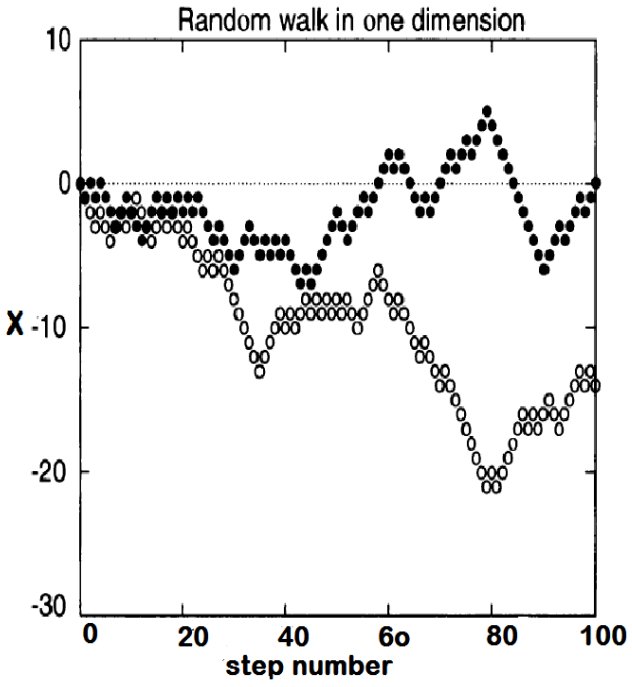

Figure 3 Random walk in one dimension(two different trials)[21].

The diffusional motion of a random walk simulation can be observed by calculating the average squared distance from the origin, $\langle x^2 \rangle$. To do this, many individual random walk simulations are carried out, and the average is taken over many individual random walkers. Results for $\langle x^2 \rangle$ versus time for a random walk in one dimension are shown in figure 4 below[21].

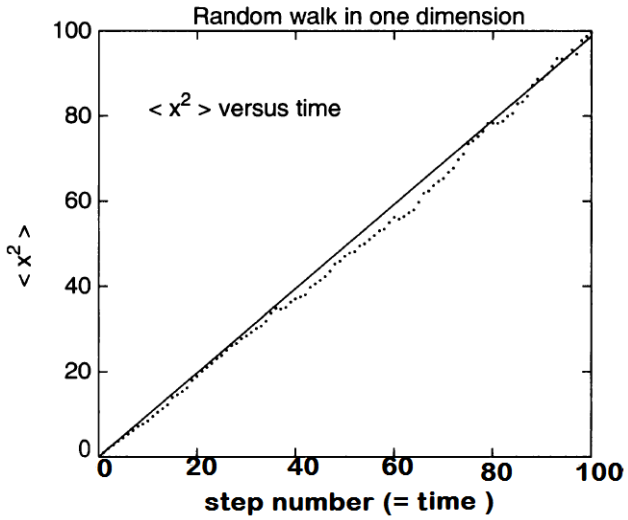

Figure 4 $\langle x^2 \rangle$ *versus step numbers(time) for random walk in one dimension[21].*

The results presented in figure 4 illustrate that diffusional behavior is observed. That is, the system follows the equation

$$\langle x^2 \rangle \propto Dt \quad \text{..... (19)}$$

Where D is the diffusion coefficient and t is time (proportional to the number of steps) [21].

CHAPTER - 3

3. MOIRÉ FRINGES AND DEFELECTOMETRY

3.1 Basic Physical Optics

3.1.1 Interference

Optical interference corresponds to the interaction of two or more light waves yielding a resultant irradiance that deviates from the sum of the component irradiances [22]. Figure 5 shows the general setup for producing interference with coherent light from two slits S_1 and S_2. The source S_0 is a monochromatic point source of light whose spherical wave fronts (circular in the drawing) fall on the two slits to create secondary sources S_1 and S_2. Spherical waves radiating out from the two secondary sources S_1 and S_2 maintain a fixed phase relationship with each other as they spread out and overlap on the screen, to produce a series of alternate bright and dark regions. The alternate regions of bright and dark are referred to as interference fringes [23].

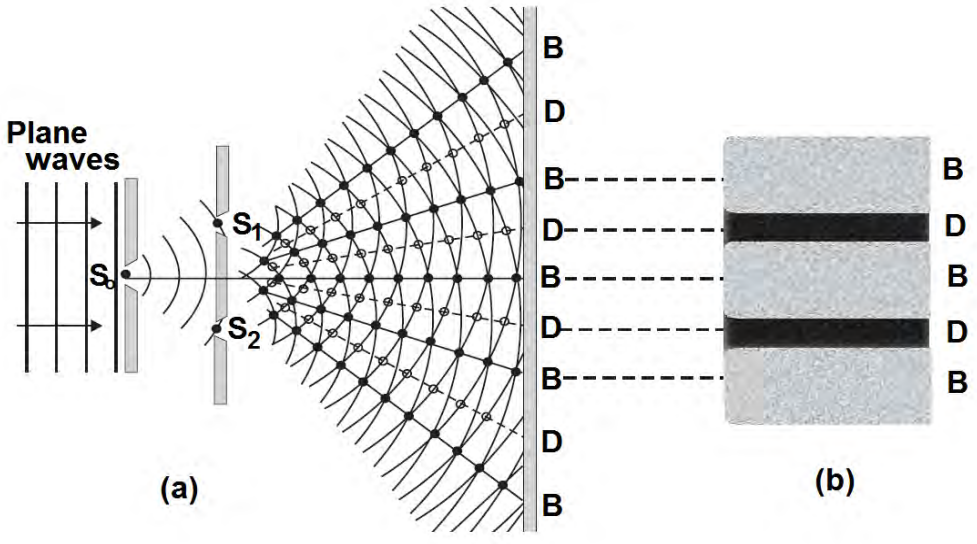

Figure 5 Young's double-slit interference experiment showing[23].
(a) General setup and (b) Typical interference fringes

With the help of the principle of superposition, it is possible to calculate the positions of the alternate maxima (bright regions) and minima (dark regions) shown in figure 5 using the following conditions on figure 6 shown below:

(a) Light from slits S_1 and S_2 is coherent; that is, there exists a fixed phase relationship between the waves from the two sources.

(b) Light from slits S_1 and S_2 is of the same wavelength.

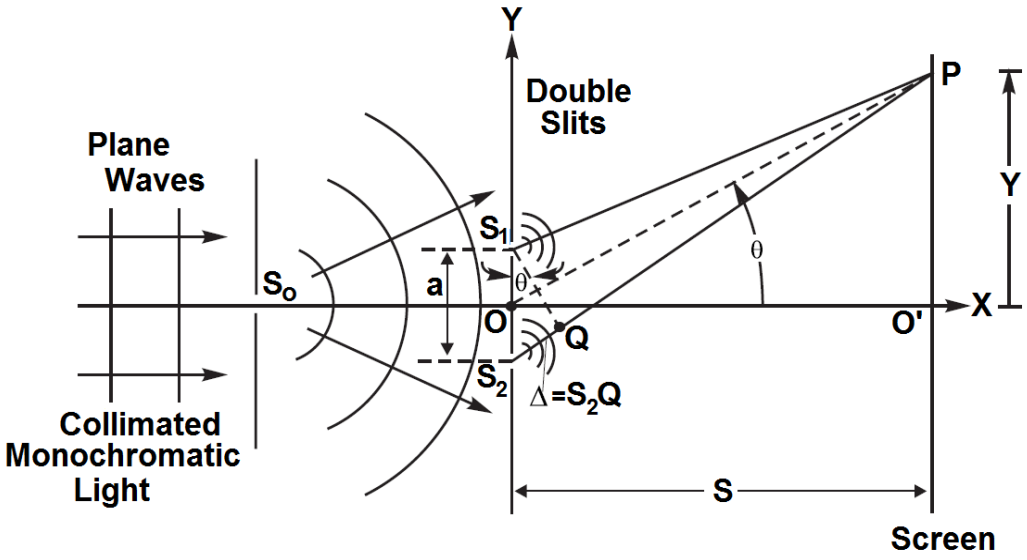

Figure 6 Young's double-slit interference experiment showing. Source S_0 is generally a small hole or narrow slit; sources S_1 and S_2 are generally long, narrow slits perpendicular to the page[23].

In figure 6 light waves from S_1 and S_2 spread out and overlap at an arbitrary point P on the screen. If the overlapping waves are in phase, we expect a bright spot at P; if they are out of phase, we expect a dark spot. So the phase difference between the two waves arriving at point P is a key factor in determining what happens there. We shall express the phase difference in terms of the path difference, which we can relate to the wavelength λ.

For clarity, figure 6 is not drawn to scale. It will be helpful in viewing the drawing to know that, in practice, the distance s from the slits to the screen is about one

meter, the distance a between slits is less than a millimeter, so that the angle θ in triangle S_1S_2Q, or triangle OPO′, is quite small. And on top of all this, the wavelength of light is a fraction of a micrometer.

The path difference Δ between S_1P and S_2P, as seen in figure 6 is given by equation (20), since the distances PS_1 and PQ are equal and since $\sin\theta = \Delta/a$ in triangle S_1S_2Q.

$$\Delta = S_2P - S_1P = S_2Q = a\sin\theta \qquad \text{..... (20)}$$

If the path difference Δ is equal to λ or some integral multiple of λ, the two waves arrive at P in phase and a bright fringe appears there (constructive interference). The condition for bright (B) fringes is, then,

$$\Delta_B = a\sin\theta = m\lambda \quad \text{where} \quad m = 0,\pm1,\pm2,..... \qquad \text{.....} \quad (21)$$

The number m is called the order number. The central bright fringe at $\theta = 0$ (point 0′ on the screen) is called the zeroth-order maximum ($m = 0$). The first maximum on either side, for which $m = \pm1$, is called the first-order maximum, and so on.

If, on the other hand, the path difference at P is an odd multiple of $\lambda/2$, the two waves arrive out of phase and create a dark fringe (destructive interference). The condition for dark (D) fringes is given by equation (22).

$$\Delta_D = a\sin\theta = \left(m + \frac{1}{2}\right)\lambda \quad \text{where } m = 0,\pm1,\pm2,..... \qquad \text{.....} \quad (22)$$

Since the angle θ exists in both triangles S_1S_2Q and OPO′, we can find an expression for the positions of the bright and dark fringes along the screen. Because θ is small, as mentioned above, we know that $\sin\theta \cong \tan\theta$, so that for triangle OPO′ we can write

$$\sin\theta \cong \tan\theta = Y/\lambda s \qquad \text{.....(23)}$$

Combining equation (23) with equations (21) and (22) in turn, by substituting for $\sin\theta$ in each, we obtain expressions for the position Y of bright and dark fringes on the screen.

$$Y_B = \frac{\lambda s}{a} m \quad \text{where } m = 0,\pm1,\pm2,..... \qquad \text{..... (24)}$$

$$Y_D = \frac{\lambda s}{a}\left(m + 1/2\right) \quad \text{where } m = 0,\pm1,\pm2,..... \qquad \text{..... (25)}$$

"How does the brightness (intensity) of the fringes vary as we move, in either direction, from the central bright fringe ($m = 0$)?" We obtain a satisfactory answer to this question by representing the two separate electric fields at point P, the one coming from S_1 as $E_1 = E_o \sin\left(\frac{2\pi}{T}\right)t$ and the one from S_2 as $E_2 = E_o \sin\left(\frac{2\pi}{T}t + \delta\right)$. The waves are assumed to have the same amplitude E_o. Here δ is the phase angle difference between the two waves arriving at P. The path difference Δ is related to the phase angle δ by the relationship

$$\frac{\delta}{\Delta} = \frac{2\pi}{\lambda} \qquad \text{..... (26)}$$

So that if $\Delta = \lambda$, $\delta = 2\pi \ \ rad = 360°$, if $\Delta = \lambda/2$, $\delta = \pi \ \ rad = 180°$, and so on.

Then, by using the principle of superposition, we can add the two electric fields at point P to obtain $E_{RES} = E_1 + E_2$. (Carrying out this step involves some trigonometry, the details of which can be found in most optics texts.) Since the intensity I of the light goes as the square of the electric field E, we square E_{RES} and average the result over one cycle of wave oscillation at P, obtaining, finally, an expression for the average intensity, I_{AV}.

$$I_{AV} = I_o \cos^2\frac{\delta}{2} \qquad \text{.....(27)}$$

Here δ is the critical phase angle difference at point P. For all points P for which $\delta = 0, 2\pi, 4\pi,$ and so on, corresponding to $\Delta = 0, \lambda, 2\lambda,$ etc., $\cos^2 \frac{\delta}{2} = 1$ and $I_{AV} = I_o$, the maximum possible "brightness." At these points, bright fringes form. For $\delta = \pi, 3\pi, 5\pi,$ and so on, corresponding to $\Delta = \lambda/2, 3\lambda/2, 5\lambda/2,$ etc. $\cos^2 \frac{\delta}{2} = 0$ and dark fringes form. The maximum intensity I_0 is equal to $(E_0 + E_0)^2$ or $4E_0^2$, since each wave has amplitude E_0. Further, from equations (26) and (20), we see that

$$\delta = \frac{2\pi}{\lambda}\Delta = \frac{2\pi}{\lambda} a \sin\theta \quad \text{..... (28)}$$

So that the phase angle δ is connected clearly through the angle θ to different points P on the screen. Going one step further, replacing $\sin\theta$ by y/s in equation (28), we have the connection between δ and any position y on the screen, such that:

$$\delta = \frac{2\pi a}{\lambda s} y \quad \text{..... (29)}$$

With equation (29) and $I_0 = 4E_0^2$, we can rewrite equation (27) in a form that relates I_{AV} directly to a position Y on the screen [24].

$$I_{AV} = 4E_0^2 \cos^2\left(\frac{\pi a}{\lambda s} y\right) \quad \text{.....(30)}$$

Where: I_{AV} = intensity of light along screen at position y
E_0 = amplitude of light wave from S_1 or S_2
s = distance from the plane of the double slit to the screen
a = slit separation
λ = wavelength of monochromatic light
y = distance above (or below) central bright fringe on the screen

3.1.2 Diffraction

The ability of light to bend around corners, a consequence of the wave nature of light, is fundamental to both interference and diffraction. Diffraction is simply any deviation from geometrical optics resulting from the obstruction of a wave front of light by some obstacle or some opening. Diffraction occurs when light waves pass through small openings, around obstacles, or by sharp edges. Several common diffraction patterns for He-Ne laser light are shown in figure 7 below [23].

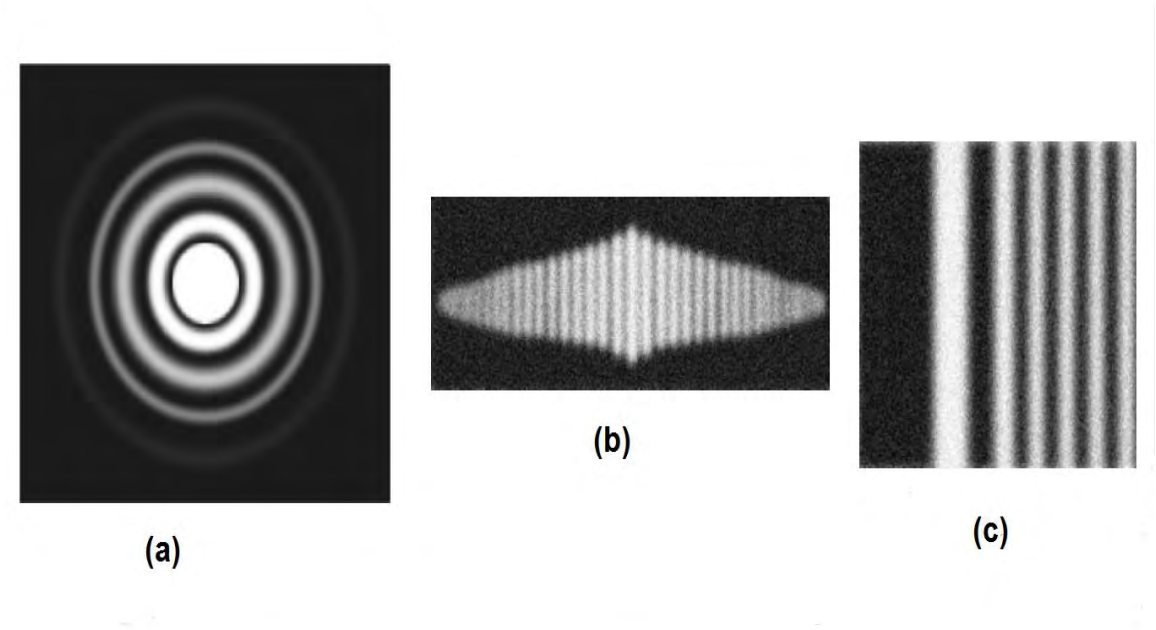

Figure 7 A typical diffraction pattern showing, light wave[23].
(a) Passing through a circular pinhole
(b) Passing through a narrow (vertical) slit and
(c) A typical pattern for diffraction by a sharp edge.

3.1.3 Diffraction Grating

An aperture with thousands of adjacent slits, is called transmission diffraction grating. The width of a single slit the opening is given by d, and the distance between slit centers is given by l (see figure 8). For clarity, only a few of the

thousands of slits normally present in a grating are shown. Note that the spreading of light occurs always in a direction perpendicular to the direction of the long edge of the slit opening that is, since the long edge of the slit opening is vertical in figure 8 the spreading is in the horizontal direction along the screen.

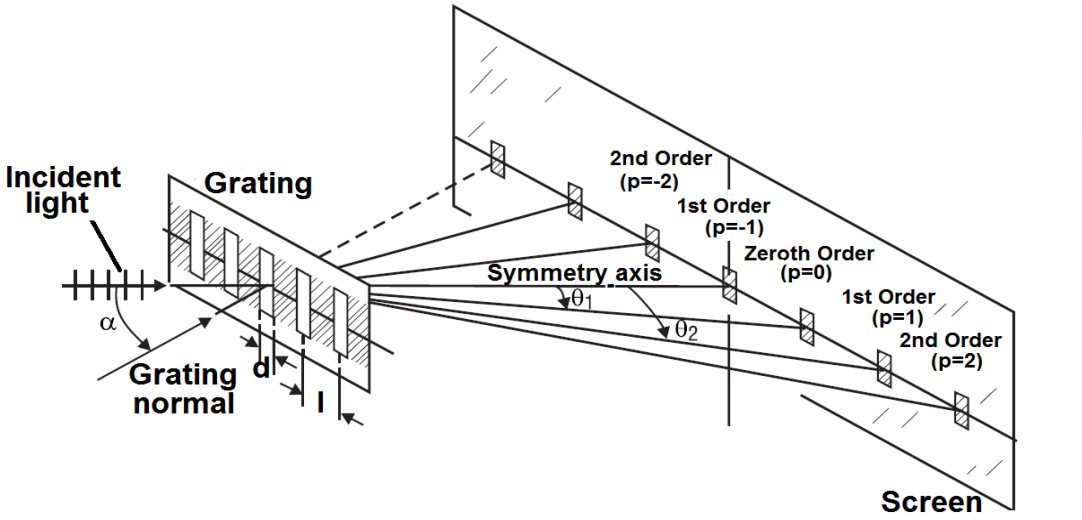

Figure 8 Diffraction of light through a grating[23].

The resulting diffraction pattern is a series of sharply defined, widely spaced fringes, as shown. The central fringe, on the symmetry axis, is called the zeroth-order fringe. The successive fringes on either side are called 1st order, 2nd order, etc., respectively. They are numbered according to their positions relative to the central fringe, as denoted by the letter p .

The intensity pattern on the screen is a superposition of the diffraction effects from each slit as well as the interference effects of the light from all the adjacent slits. The combined effect is to cause overall cancellation of light over most of the screen with marked enhancement over only limited regions, as shown in figure 8. The location of the bright fringes is given by the following expression, called the grating equation, assuming that Fraunhofer conditions hold [23].

$$l\left(\sin\alpha+\sin\theta_p\right)=p\lambda \quad \text{where} \quad p=0,\pm1,\pm2,.... \qquad \ldots\ldots\ldots\ldots\ldots\ldots (31)$$

Where l = distance between slit centers

α = angle of incidence of light measured with respect to the normal to the grating surface

θ_p = angle locating the p[th]-order fringe

p = an integer taking on values of $0,\pm1,\pm2,....$, etc.

λ = wavelength of light

Note that, if the light is incident on the grating along the grating normal ($\alpha = 0$), the grating equation, equation (31), reduces to the more common form shown in equation (32).

$$l(\sin\theta_p) = p\lambda \quad \text{.....(32)}$$

If, for example, you shine a He-Ne laser beam perpendicularly onto the surface of a transmission grating, you will see a series of brilliant red dots, spread out as shown in figure.8. A complete calculation would show that less light falls on each successively distant red dot or fringe, the $p = 0$ or central fringe being always the brightest. Nevertheless, the location of each bright spot, or fringe, is given accurately by equation (31) for either normal incidence ($\alpha = 0$) or oblique incidence ($\alpha \neq 0$). If light containing a mixture of wavelengths (white light, for example) is directed onto the transmission grating, equation (31), holds for each component color or wavelength. So each color will be spread out on the screen according to equation (31), with the longer wavelengths (red) spreading out farther than the shorter wavelengths (blue). In any case, the central fringe ($p = 0$) always remains the same color as the incident beam, since all wavelengths in the $p = 0$ fringe have θ_p, hence all overlap to re-form the "original" beam and therefore the original "color"[23].

3.2 What is Moiré?

The term "Moiré" is not the name of a person; in fact, it is a French word referring to "an wavy finish usually produced on a fabric by pressing between engraved rollers" (Webster's 1981). In optics it refers to a beat pattern produced between two gratings of approximately equal spacing. It can be seen in everyday things

such as the overlapping of two window screens, the rescreening of a half-tone picture, or with a striped shirt seen on television. The use of moiré for reduced sensitivity testing was introduced by Lord Rayleigh in 1874. Lord Rayleigh looked at the moiré between two identical gratings to determine their quality even though each individual grating could not be resolved under a microscope.

Moiré patterns are extremely useful to help understand basic interferometry and interferometric test results. Figure 9 shows the moiré pattern (or beat pattern) produced by two identical straight-line gratings rotated by a small angle relative to each other. A dark fringe is produced where the dark lines are out of step one-half period, and a bright fringe is produced where the dark lines for one grating fall on top of the corresponding dark lines for the second grating. If the angle between the two gratings is increased, the separation between the bright and dark fringes decreases[24].

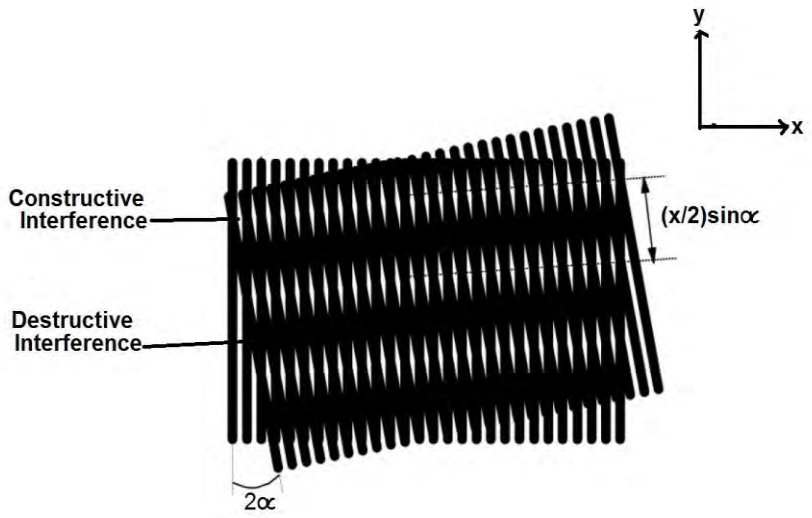

Figure 9 Moiré between two straight-line gratings of the same pitch at an angle α with respect to one another.

If the gratings are not identical straight-line gratings, the moiré pattern (bright and dark fringes) will not be straight equi-spaced fringes. The following analysis shows how to calculate the moiré pattern for arbitrary gratings. Let the intensity transmission function for two gratings $f_1(x, y)$ and $f_2(x, y)$ be given by

$$\left.\begin{aligned} f_1(x,y) &= a_1 + \sum_{n=1}^{\infty} b_{1n}\cos[n\phi_1(x,y)], \\ f_2(x,y) &= a_2 + \sum_{m=1}^{\infty} b_{2m}\cos[m\phi_2(x,y)] \end{aligned}\right\} \quad \text{.....(33)}$$

Where $\phi(x,y)$ is the function describing the basic shape of the grating lines.

For the fundamental frequency, at the center of each bright line

$$\phi(x,y) = 2\pi n \quad \text{..... (34)}$$

and at the center of each dark line

$$\phi(x,y) = 2\pi(n+\tfrac{1}{2}) \quad \text{..... (35)}$$

The b coefficients determine the profile of the grating lines (i.e., square wave, triangular, sinusoidal, etc.) For a sinusoidal line profile, b_{i1} is the only nonzero term. When these two gratings are superimposed, the resulting intensity transmission function is given by the product

$$f_1(x,y)\,f_2(x,y) = a_1a_2 + a_1\sum_{m=1}^{\infty} b_{2m}\cos[m\phi_2(x,y)] \quad + a_2\sum_{n=1}^{\infty} b_{1n}\cos[n\phi_1(x,y)]$$

$$+ \sum_{m=1}^{\infty}\ \sum_{n=1}^{\infty} b_{1n}b_{2m}\cos[n\phi_1(x,y)]\cos[m\phi_2(x,y)] \quad \text{..... (36)}$$

The first three terms of equation (36) provide information that can be determined by looking at the two patterns separately. The last term is the interesting one, and can be rewritten as:

$$\sum_{m=1}^{\infty}\ \sum_{n=1}^{\infty} b_{1n}b_{2m}\cos[n\phi_1(x,y)]\cos[m\phi_2(x,y)] \ =$$

$$\frac{1}{2}b_{11}b_{21}\cos[\phi_1(x,y) - \phi_2(x,y)]$$

$$+ \ \frac{1}{2}\sum_{m=1}^{\infty}\ \sum_{n=1}^{\infty} b_{1n}b_{2m}\cos[n\phi_1(x,y) - m\phi_2(x,y)]; n = m \neq 1$$

$$+ \ \frac{1}{2}\sum_{m=1}^{\infty}\ \sum_{n=1}^{\infty} b_{1n}b_{2m}\cos[n\phi_1(x,y) - m\phi_2(x,y)]x \quad \text{.....(37)}$$

This expression shows that by superimposing the two gratings, the sum and difference between the two gratings is obtained. The first term of equation (37) represents the difference between the fundamental pattern masking up the two gratings. It can be used to predict the moiré pattern shown in figure 9. Assuming

that two gratings are oriented with an angle 2α between them with the $y-axis$ of the coordinate system bisecting this angle, the two grating functions $\phi_1(x,y)$ and $\phi_2(x,y)$ can be written as:

$$\left.\begin{aligned}\phi_1(x,y) &= \frac{2\pi}{\lambda_1}\left(x\cos\alpha + y\sin\alpha\right)\\ \phi_2(x,y) &= \frac{2\pi}{\lambda_2}\left(x\cos\alpha - y\sin\alpha\right)\end{aligned}\right\} \quad \text{..... (38)}$$

where λ_1 and λ_2 are the line spacings of the two gratings and equation (38) can be rewritten as

$$\phi_1(x,y) - \phi_2(x,y) = \frac{2\pi}{\lambda_{beat}} x\cos\alpha + \frac{4\pi}{\bar{\lambda}} y\sin\alpha \quad \text{..... (39)}$$

Where $\bar{\lambda}$ is the average line spacing, λ_{beat} and is the beat wavelength between the two gratings given by

$$\lambda_{beat} = \frac{\lambda_1\lambda_2}{\lambda_2 - \lambda_1} \quad \text{..... (40)}$$

Using equation (37), the moiré or beat will be lines whose centers satisfy the equation

$$\phi_1(x,y) - \phi_2(x,y) = M2\pi \quad \text{..... (41)}$$

Three separate cases for moiré fringes can be considered. When $\lambda_1 = \lambda_2 = \lambda$, the first term of equation (39) is zero, and the fringe centers are given by

$$M\lambda = 2y\sin\alpha \quad \text{.....(42)}$$

Where M is an integer corresponding to the fringe order. As was expected, equation (42) is the equation of equi-spaced horizontal lines as seen in figure 9 The other simple case occurs when the gratings are parallel to each other with $\alpha = 0$. This makes the second term of equation (39) vanish. The moiré will then be lines that satisfy

$$M\lambda_{beat} = x \quad \text{..... (43)}$$

These fringes are equally spaced, vertical lines parallel to the y axis. For the more general case where the two gratings have different line spacings and the angle between the gratings is nonzero, the equation for the moiré fringes will

now be

$$M\bar{\lambda} = x\cos\alpha + 2y\sin\alpha \quad \text{.....(44)}$$

This is the equation of straight lines whose spacing and orientation is dependent on the relative difference between the two grating spacings and the angle between the gratings. Figure 10 shows moiré patterns for these three cases.

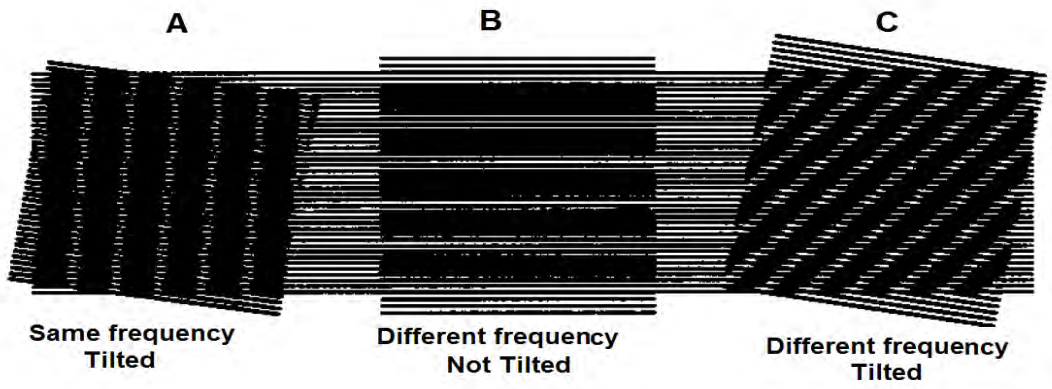

Figure 10 Moiré patterns caused by two straight-line gratings with;
(A) The same pitch tilted with respect to one another,
(B) Different frequencies and no tilt, and
(C) Different frequencies tilted with respect to one another.

The orientation and spacing of the moiré fringes for the general case can be determined from the geometry shown in figure 11(Chiang, 1983). The distance AB can be written in terms of the two grating spacings;

$$\overline{AB} = \frac{\lambda_1}{\sin(\theta - \alpha)} = \frac{\lambda_2}{\sin(\theta + \alpha)} \quad \text{..... (45)}$$

Where θ is the angle the moiré fringes make with the y axis.

After rearranging, the fringe orientation angle θ is given by

$$\tan\theta = \tan\alpha\left(\frac{\lambda_1 + \lambda_2}{\lambda_2 - \lambda_1}\right) \quad \text{..... (46)}$$

When $\alpha = 0$ and $\lambda_1 \neq \lambda_2, \theta \neq 90^0$ and when $\lambda_1 = \lambda_2$ with $\alpha \neq 0, \theta = 90^0$ as expected. The fringe spacing perpendicular to the fringe lines can be found by equating quantities for the distance DE;

$$\overline{DE} = \frac{\lambda_1}{\sin 2\alpha} = \frac{C}{\sin(\theta + \alpha)} \quad \text{..... (47)}$$

Where C is the fringe spacing or contour interval. This can be rearranged to yield

$$C = \lambda_1 \left[\frac{\sin(\theta + \alpha)}{\sin 2\alpha} \right] \quad \text{..... (48)}$$

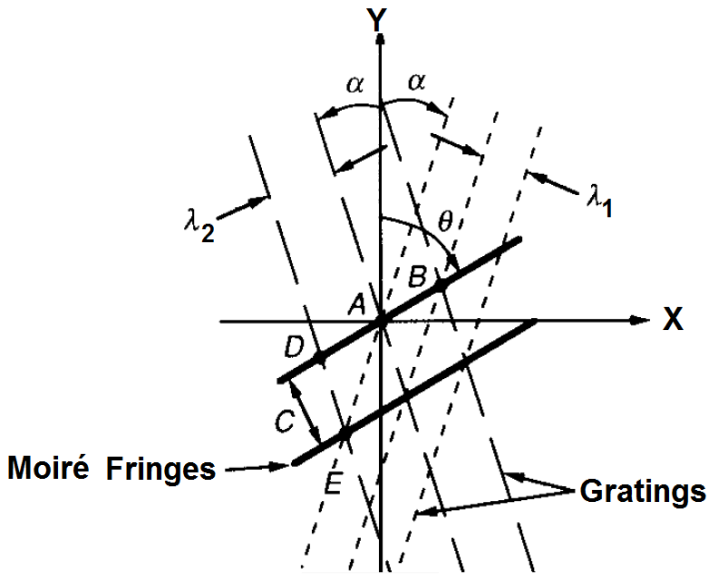

Figure 11 Geometry used to determine spacing and angle of moiré fringes between two gratings of different frequencies tilted with respect to one another[24].

By substituting for the fringe orientation θ, the fringe spacing can be found in terms of the grating spacings and angle between the gratings;

$$C = \frac{\lambda_1 \lambda_2}{\sqrt{\lambda_2^2 \sin^2 2\alpha + (\lambda_2 \cos 2\alpha - \lambda_1)^2}} \quad \text{..... (49)}$$

In the limit that $\alpha = 0$ and $\lambda_1 \neq \lambda_2$, the fringe spacing equals λ_{beat}, and in the limit that $\lambda_1 = \lambda_2 = \lambda$ and $\alpha \neq 0$, the fringe spacing equals $\lambda/(2\sin\alpha)$. It is possible to

determine λ_2 and α from the measured fringe spacing and orientation as long as λ_1 is known (Chiang 1983) [24].

3.3 Fringe Projection

Fringe projection entails projecting a fringe pattern or grating on an object and viewing it from a different direction. The first use of fringe projection for determining surface topography was presented by Rowe and Welford in 1967. It is a convenient technique for contouring objects that are too coarse to be measured with standard interferometry. Fringe projection is related to optical triangulation using a single point of light and light sectioning where a single line is projected onto an object and viewed in a different direction to determine the surface contour.

Moiré and fringe projection interferometry complement conventional holographic interferometry, especially for testing optics to be used at long wavelengths. Although two-wavelength holography (TWH) can be used to contour surfaces at any longer-than-visible wavelength, visible interferometric environmental conditions are required. Moiré and fringe projection interferometry can contour surfaces at any wavelength longer than 10-100μm with reduced environmental requirements and no intermediate photographic recording setup.

A simple approach for contouring is to project interference fringes or a grating onto an object and then view from another direction. Figure 12 shows the optical setup for this measurement. Assuming a collimated illumination beam and viewing the fringes with a telecentric optical system, straight equally spaced fringes are incident on the object, producing equally spaced contour intervals. The departure of a viewed fringe from a straight line shows the departure of the surface from a plane reference surface.

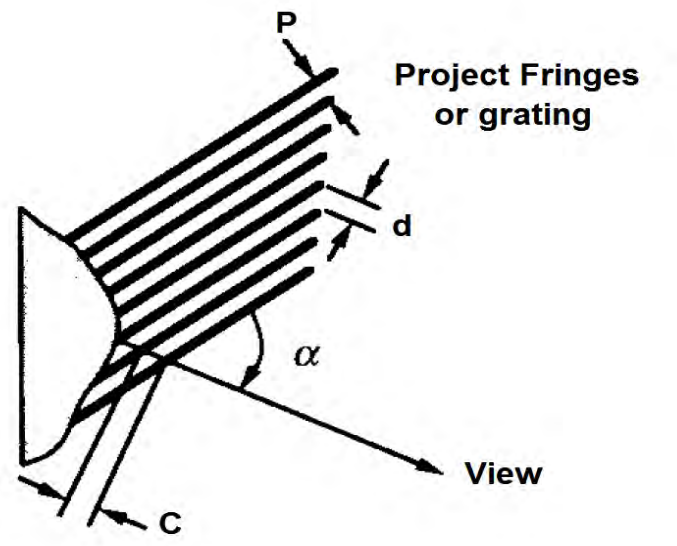

Figure 12 Projection of fringes or grating onto object and viewed at an angle . P is the grating pitch or fringe spacing and C is the contour interval[24].

When the fringes are viewed at an angle α relative to the projection direction, the spacing of the lines perpendicular to the viewing direction will be

$$d = \frac{P}{\cos\alpha} \quad \text{..... (50)}$$

The contour interval C (the height between adjacent contour lines in the viewing direction) is determined by the line or fringe spacing projected onto the surface and the angle between the projection and viewing directions;

$$C = \frac{P}{\sin\alpha} = \frac{d}{\tan\alpha} \quad \text{..... (51)}$$

These contour lines are planes of equal height, and the sensitivity of the measurement is determined by α. The larger the angle α, the smaller the contour interval. If $\alpha = 90°$, then the contour interval is equal top, and the sensitivity is a maximum. The reference plane will be parallel to the direction of the fringes and perpendicular to the viewing direction as shown in figure 13. Even though the maximum sensitivity can be obtained at 90^0, this angle between the projection and viewing directions will produce a lot of unacceptable shadows on

the object. These shadows will lead to areas with missing data where the object cannot be contoured. When $\alpha = 0$, the contour interval is infinite, and the measurement sensitivity is zero. To provide the best results, an angle no larger than the largest slope on the surface should be chosen.

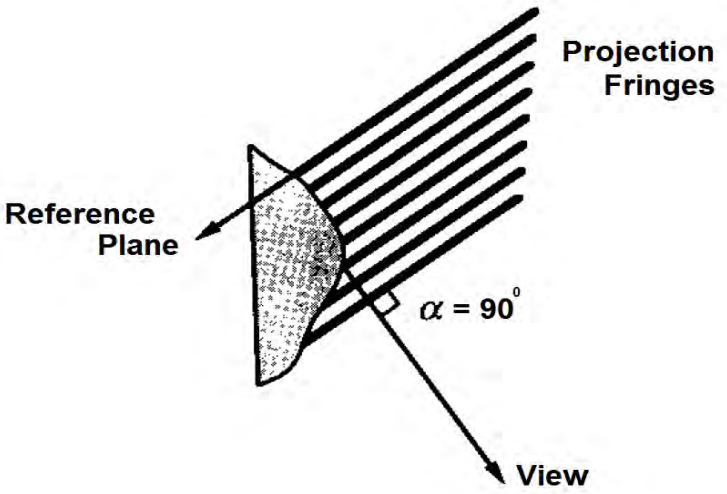

Figure 13 Maximum sensitivity for fringe projection with a 90^0 angle between projection and viewing[24].

When interference fringes are projected onto a surface rather than using a grating, the fringe spacing P is determined by the geometry shown in figure 14 and is given by

$$P = \frac{\lambda}{2\sin\Delta\theta} \qquad \text{..... (52)}$$

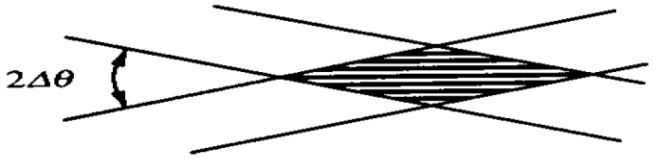

Figure 14 Fringes produced by two interfering beams[24].

Where λ is the wavelength of illumination and $2\Delta\theta$ is the angle between the two interfering beams. Substituting the expression for P into equation (51), the contour interval becomes

$$C = \frac{\lambda}{2(\sin\Delta\theta)\sin\alpha} \qquad \text{..... (53)}$$

If a simple interferometer such as a Twyman-Green is used to generate projected interference fringes, tilting one beam with respect to the other will change the contour interval. The larger the angle between the two beams, the smaller the contour interval will be [24].

3.4 Shadow Moiré

A simple method of moiré interferometry for contouring objects uses a single grating placed in front of the object as shown in Figure 15. The grating in front of the object produces a shadow on the object that is viewed from a different direction through the grating. A low-frequency beat or moiré pattern is seen.

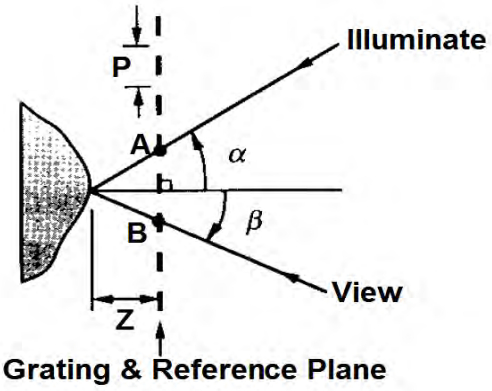

Figure 15 Geometry for shadow moiré with illumination and viewing at infinity, i.e. parallel illumination and viewing[24].

This pattern is due to the interference between the grating shadows on the object and the grating as viewed. Assuming that the illumination is collimated and that the object is viewed at infinity or through a telecentric optical system, the height z between the grating and the object point can be determined from the geometry shown in Figure 15. This height is given by

$$z = \frac{Np}{\tan\alpha + \tan\beta} \quad \text{..... (54)}$$

Where α is the illumination angle, β is the viewing angle, p is the spacing of the grating lines, and N is the number of grating lines between the points A and B (see Figure 15). The contour interval in a direction perpendicular to the grating will simply be given by

$$C = \frac{p}{\tan\alpha + \tan\beta} \quad \text{..... (55)}$$

Again, the distance between the moiré fringes in the beat pattern depends on the angle between the illumination and viewing directions. The larger the angle, the smaller the contour interval. If the high frequencies due to the original grating are

filtered out, then only the moiré interference term is seen. The reference plane will be parallel to the grating. Note that this reference plane is tilted with respect to the reference plane obtained when fringes are projected onto the subject. Essentially, the shadow moiré technique provides a way of removing the “tilt” term and repositioning the reference plane. The contour interval for shadow moiré is the same as that calculated for projected fringe contouring (equation 51) when one of the angles is zero with $d = p$.

Most of the time, it is difficult to illuminate an entire object with a collimated beam. Therefore, it is important to consider the case of finite illumination and viewing distances. It is possible to derive this for a very general case (Meadows et al. 1970; Takasaki 1970; Bell 1985); however, for simplicity, only the case where the illumination and viewing positions are the same distance from the grating will be considered. Figure 16 shows a geometry where the distance between the illumination source and the viewing camera is given by w, and the distance between these and the grating is l. The grating is assumed to be close enough to the object surface so that diffraction effects are negligible in this case the height between the object and the grating is given by

$$z = \frac{Np}{\tan\alpha' + \tan\beta'} \qquad \text{..... (56)}$$

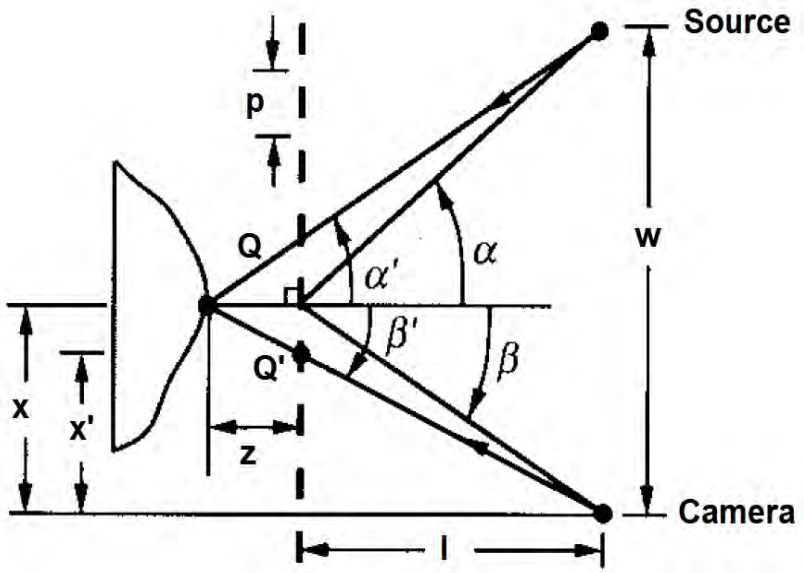

Figure 16 Geometry for shadow moiré with illumination and viewing at finite distances [24].

Where α' and β' are the illumination and viewing angles at the object surface. These angles change for every point on the surface and are different from α and β in figure 16, where a and b are the illumination and viewing angles at the grating (reference) surface. The surface height can also be written as (Meadows et al. 1970; Takasaki 1973; Chiang 1983)

$$z = NC(z) = \frac{Np(l+z)}{w} = \frac{Npl}{w - lp} \quad \text{..... (57)}$$

This equation indicates that the height is a complex function depending on the position of each object point. Thus, the distance between contour intervals is dependent on the height of the surface and the number of fringes between the grating and the object. Individual contour lines will no longer be planes of equal height. They are now surfaces of equal height. The expression for height can be simplified by considering the case where the distance to the source and viewer is

large compared to the surface height variations $l >> z$. Then the surface height can be expressed as

$$z = \frac{Npl}{w} = \frac{Np}{\tan\alpha + \tan\beta} \quad \text{..... (58)}$$

Even though the angles α and β vary from point-to-point on the surface, the sum of their tangents remains equal to w/l for all object points as long as $l >> z$. The contour interval will be constant in this regime and will be the same as that given by equation (55). Because of the finite distances, there is also distortion due to the viewing perspective. A point on the surface Q will appear to be at the location Q' when viewed through the grating. By similar triangles, the distances x and x' from a line perpendicular to the grating intersecting the camera location can be related using

$$\frac{x}{z+l} = \frac{x'}{l} \quad \text{..... (59)}$$

Where x and x' are defined in figure 16. Equation (59) can be rearranged to yield the actual coordinate x in terms of the measured coordinate x' and the measurement geometry,

$$x = x'\left(1 + \frac{z}{l}\right) \quad \text{..... (60)}$$

Likewise, the y coordinate can be corrected using

$$y = y'\left(1 + \frac{z}{l}\right) \quad \text{.....(61)}$$

This enables the measured surface to be mapped to the actual surface to correct for the viewing perspective. These same correction factors can be applied to fringe projection [24].

3.5 Projection Moiré

Moiré interferometry can also be implemented by projecting interference fringes or a grating onto an object and then viewing through a second grating in front of the viewer (see figure 17). The difference between projection and shadow moiré is that two different gratings are used in projection moiré. The orientation of the reference plane can be arbitrarily changed by using different grating pitches to view the object. The contour interval is again given by equation (55),

$$C = \frac{d}{\tan\alpha + \tan\beta} \qquad \text{.....(62)}$$

Where d is the period of the grating in the y plane, as long as the grating pitches are matched to have the same value of d. This implementation makes projection moiré the same as shadow moiré, although projection moiré can be much more complicated than shadow moiré. A good theoretical treatment of projection moiré is given by Benoit et al. (1975) [24].

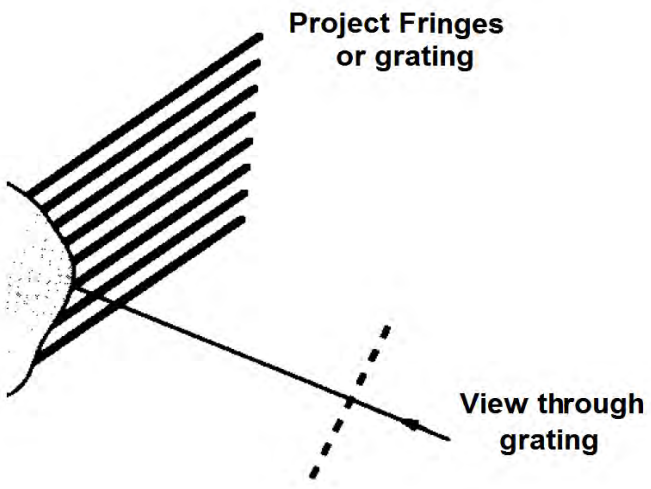

Figure 17 **Projection moiré where fringes or a grating are projected onto a surface and viewed through a second grating***[24].*

3.6 Moiré Defelectometry

Moiré deflectometry (MD) is a simple optical testing technique for phase objects and specular surfaces based on the moiré effect. The method provides a light ray deflection mapping caused by a phase object or reflection in a surface. From this information the refractive index region or surface quality is obtained. The MD could be more attractive than interferometric techniques because a great mechanical stability is not required and its alignment is easier. Interferometry is also limited by the source's temporal coherence, which has a narrow spectral width; while MD requires mainly a high spatial coherence so a well collimated light beam is necessary. For optical materials, direct birefringence measurements have been reported using MD. In microscopy, MD has been used for phase objects detection. Moiré deflectometry also has been used to find temperature distribution in flames and for mapping hot objects. A typical moiré deflectometer consists of two identical Ronchi gratings (G_1,G_2) of period p separated distance Δ and illuminated by a collimated He-Ne laser beam as shown below [6,25,26].

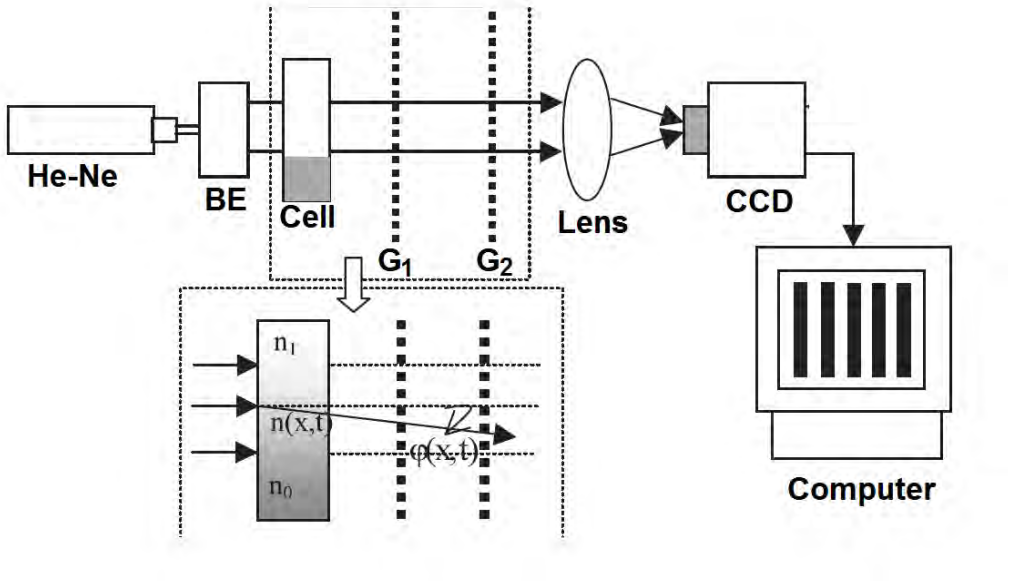

Figure 18 The experimental set-up for measuring diffusion coefficient in transparent liquid mixtures by using the Moiré deflectometry technique[6].

3. 6.1 Moiré Defelectometry and index of refraction

As explained above a conventional moiré deflectometer consists of two identical Ronchi gratings, a collimated light source, and a diffusing screen attached to the output grating. A schematic of the system is shown in figure 19. The gratings are shown separated by a distance Δ , and their lines are rotated relative to each other by a small angle θ. When a collimated light beam passes through the gratings, a moiré pattern is produced on the screen. The pattern consists of straight fringes perpendicular to the original grating lines, separated by a distance of p'.

$$P' = \frac{P}{2\sin(\theta/\ 2)} \approx \frac{P}{\theta} \quad \text{.....(63)}$$

Where p is the pitch of the gratings.

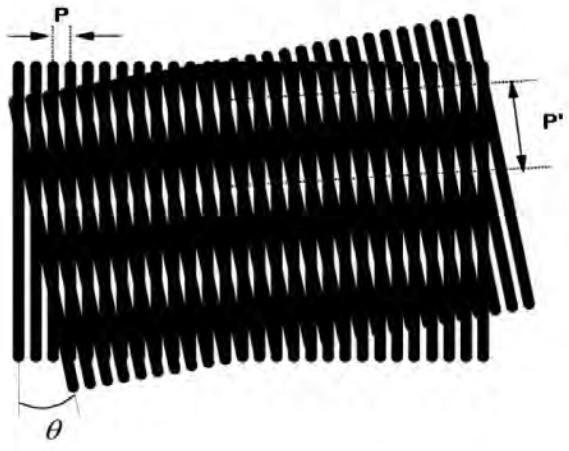

Figure 19 A moiré pattern, formed by superimposing two sets of parallel lines, one set rotated by an angle θ with respect to the other[25].

The moiré effect for a small grating-separation distance can be explained by pure geometrical optics. However, when the grating separation increases, diffraction introduces undesired effects that limit the performance of the system. To minimize these effects, the distance Δ between the gratings must be exactly one of the Fourier image planes of the gratings, namely

$$\Delta_l = l\frac{p^2}{\lambda} \quad , \; l = 1,2,3,..... \qquad \text{.....(64)}$$

For these distances the fringe contrast will be maximum.

$$\text{When } \Delta = \left(l + \frac{1}{2}\right)\frac{p^2}{\lambda} \qquad \text{..... (65)}$$

the fringes will vanish completely. In equations (64) and (65), λ is the wavelength of the collimated light beam.

If the collimated light is refracted by a phase object before entering the deflectometer, the original straight parallel moiré fringes will be distorted. $\phi_x(r)$, the angle of refraction in the x - direction at a point $r \equiv x, y$, is related to the fringe shift $\delta h_y(r)$ in the y - direction by:

$$\phi_x(r) = \frac{\theta \delta h_y(r)}{\Delta} = \frac{P \delta h_y(r)}{P'\Delta} \qquad \text{.....(66)}$$

By measuring $\delta h_y(r)$, $\phi_x(r)$ can be calculated. In turn, the x component of the index-of-refraction gradient may be calculated by using the equation

$$\phi_x(r) = \frac{1}{n_f}\int_{z_0}^{z_f} \frac{\partial n(r)}{\partial x} dz \qquad \text{.....(67)}$$

$$\text{or} \qquad \phi_x(r) = \frac{G}{n_f}\int_{z_0}^{z_f} \frac{\partial \rho(r)}{\partial x} dz \qquad \text{..... (68)}$$

Where z_o and z_f are the boundaries of the phase object along the line of sight and n is the index of refraction, which is related to the density ρ by

$$n - 1 = G\rho \qquad \text{..... (69)}$$

Where the coefficient G is the Gladstone-Dale constant, a function of the wavelength λ. For air, at a wavelength of $\lambda = 6328A^0$, $G = 0.227cm^3/g$. n_f is the index of refraction of the medium surrounding the object [25].

3.6.2 Moiré Defelectometry and Diffusion Coefficient

In the Moiré Defelectometery experiment the deflected laser beam due to changes in refractive index in the diffusion cell yields the shifted self-images of the gratings, and resultant Moiré fringes show a deviation. For an isothermal mixture, without generation and recombination, the physical problem associated with the experiment can be formulated mathematically.

For a diffusion column of constant cross section, extended in the $x-direction$, and with concentration varying with the position coordinate x only. By considering the column as a semi-infinite medium since the diffusion process is very slow, the boundary condition at the open end of the column does not influence the solution during the time range of interest. Thus, the diffusion process can be formulated in terms of a one-dimensional problem [6].

The free diffusion process is governed by Fick's second law, and for one-dimensional diffusion along $x-axis$ it is given by [1].

$$\frac{\partial c(x,t)}{\partial t} = D\frac{\partial^2 c(x,t)}{\partial x^2} \qquad \text{..... (70)}$$

Where $c(x,t)$ is the concentration at x at time t, D is the diffusion coefficient, assumed to be independent of concentration, and x is the direction of diffusion. Furthermore, if there is a net external force, F (e.g. gravitational force), acting in the $x-direction$ upon the dissolved molecules and if μ be the mobility of the molecules under consideration (i.e. the steady velocity, acquired under the action of unit force), the steady velocity of these molecules would be $F\mu$, and the

resulting flux of matter would be $c(x,t)F\mu$ Consequently the rate of the concentration changes would be:

$$\frac{\partial c(x,t)}{\partial t} = D\frac{\partial^2 c(x,t)}{\partial x^2} - \mu F\frac{\partial c(x,t)}{\partial x} \quad \text{.................................... (71)}$$

It is even possible to reduce the problem of equation (71) to that of ordinary diffusion equation (1), by means of the following transformation [20]:

$$c(x,t) = c*(x,t)\exp\left[-\frac{\mu F}{2D}x - \frac{\mu^2 F^2}{4D}t\right] \quad \text{.............................. (72)}$$

Where $c*(x,t)$ is a function that satisfies equation (70). Hence there are no difficulties in treating problems of this type. On the other hand, if the steady velocity of the dissolved molecules (μF) is very slow, the current due to the external forces can be neglected and equation (71) reduces to equation (70).

The solution of equation (70), for two binary liquid mixtures initially $(t=0)$ separated at $x=0$ with concentrations c_1 and c_2 is an error function [1, 20]

$$c(x,t) = \frac{c_o - c_1}{2} + \frac{c_o - c_1}{2}erf\left[\frac{x}{2\sqrt{Dt}}\right] \quad \text{.................................(73)}$$

The error function is defined by [27]

$$erf = \frac{2}{\sqrt{\pi}}\int_0^x e^{-t^2}dt \quad \text{...(74)}$$

On the other hand, if we consider the solution of equation (71), in equation (73) x is replaced by $x - \mu g t$ [20]. In this case, the influence of gravity causes a change in the central diffusion location, that is, another layer as the second centre of diffusion will form this effect is called baro-diffusion effect [28].

In a transparent mixture, a change in the concentration produces a change of the refractive index, which, for small concentration gradients, can be considered a linear function between refractive index and concentration. Then we can write, for the refractive index gradient [20].

$$\frac{\partial n(x,t)}{\partial x} = \frac{n_0 - n_1}{2\sqrt{\pi D t}} \exp\left[-\frac{x^2}{4Dt} \right] \quad \text{..... (75)}$$

Where $n(x,t)$ is the local refractive index at time t in the diffusion cell, n_o the refractive index of the high concentration solution and n_1 that of the low concentration solution. If the refractive index changes, the rays contributing to the formation of the Moiré fringes pattern will be deflected locally according to refractive index distribution, accordingly the Moiré fringes will also change.

The incident parallel laser beam, passing through the diffusion cell, bends by angle $\varphi(x,t)z_t$, depending on the distribution of the refractive index on the cell. Because the refractive index (concentration) depends on time t and x, accordingly, the deflection angle also would be time and position dependent. Due to the deflection of the collimated beam, impinging on the deflectometry system, the Fourierimage of the first grating shifts on the second grating. For small bending of light rays, the amount of Fourier image shift would be $\varphi(x,t)z_t$. The displacement of the Fourier image of the first grating on the second one, cause the Moiré fringe to shift with respect to the original locations. The amount of fringe shift, $\Delta\xi(x,t)$ is given by [10].

$$\Delta\xi(x,t) = \frac{z_t}{\theta}\varphi(x,t) \quad \text{..... (76)}$$

Where θ is a small tilt angle between the intersections of the grating lines and z_t is the t^{th} Talbot distance between gratings. The desired information from diffusion process is contained in $\varphi(x,t)z_t$. On the other hand, the relation between the integrated deflection angle and the local refractive index $n(x,t)$, is given by [18]

$$\Delta\varphi(x,t)=\frac{1}{n_a}\int_0^L\left[\frac{\partial n(x,y,z,t)}{\partial x}\right]_{y=cont}dz \qquad \text{..... (77)}$$

Where n_a is the ambient refractive index and the derivative denotes the lateral gradient of the refractive index along the $x-axis$ (diffusion direction) and L represents the thickness of the diffusion cell measured along the propagation axes ($z-axis$). The diffusion process is assumed to occur only along the $x-direction$, so the index of refraction along the $z-direction$ remains constant and equation (77) becomes

$$\varphi(x,t)=\frac{d}{n_a}\frac{\partial n(x,t)}{\partial x} \qquad \text{..... (78)}$$

Taking into account equation (78), equation (76) can be rewritten as

$$\Delta\xi(x,t)=\frac{z_t d}{n_a\theta}\frac{\partial n(x,t)}{\partial x} \qquad \text{.....(79)}$$

Equation (79) shows that Moiré fringes deformation is proportional to the refractive index gradient introduced by the diffusion process. By replacing equation (75) in equation (79), the corresponding local shift of the Moiré fringes results

$$\Delta\xi(x,t)=\frac{z_t d}{\theta}\frac{n_o-n_1}{2\sqrt{\pi Dt}}\exp\left[-\frac{x^2}{4Dt}\right]=\frac{\Delta_o}{\sqrt{t}}\exp\left[-\frac{x^2}{4Dt}\right] \qquad \text{..... (80)}$$

Where, for simplicity, Δ_o is defined as

$$\frac{z_t d(n_o-n_1)}{2\theta\sqrt{\pi D}}$$

Equation (80) predicts the time evaluations of Moiré fringes along the diffusion cell. It is shown that at the beginning, at distances far from the boundary layer, and also for long times, the shift of the fringes vanishes, that is, the concentration /refractive index becomes uniform along the cell.

The diffusion coefficient can be obtained from a single Moiré pattern recorded at time instant t_o. For two distances x_1 and $x_2 > x_1$, along the diffusion cell, the local shift of Moiré fringes would be:

$$\Delta_1 = \frac{\Delta_o}{\sqrt{t_0}} \exp\left[-\frac{x_1^2}{4Dt_0} \right] \text{ and } \quad \Delta_2 = \frac{\Delta_o}{\sqrt{t_0}} \exp\left[-\frac{x_2^2}{4Dt_0} \right] \quad \text{.....(81)}$$

The ratio of two local shifts is

$$\eta = \frac{\Delta_1}{\Delta_2} = \exp\left[-\frac{x_1^2 - x_2^2}{4Dt_0} \right] \quad \text{..... (82)}$$

Then the diffusion coefficient can be defined as

$$D = \frac{x_2^2 - x_1^2}{4t_0 \ln \eta} \quad \text{..... (83)}$$

CHAPTER 4

4. EXPERIMENTAL TECHNIQUES

4.1 Apparatuses

In carring out this experiment the following apparatuses were used the He-Ne laser to produce the beam, the diffusion cell (Phase Object) (figure 21), Syringes to fill the solution and water into the diffusion cell, Plastic bottles to keep different molar solutions of NaCl (figure 20), two Ranchi Gratings to produce Moiré patterns, the Mercury thermometer to measure the temperature of the room, a lens to magnify the fringes, Opal screen to observe the fringe pattern, CCD(Digital camera with 10.1Mega pixel) to take pictures from the Opal screen, a data cable to connect the digital camera with the computer and PC(laptop computer) to analyze the data.

Figure 20 Plastic bottles used to keep different molar solutions of NaCl.

Figure 21 The diffusion cell (made of two cuvettes).

4.2 Experimental Set-up

The Moiré deflectometry experimental set-up used to measure the diffusion coefficient of different salt solution in pure water at a temperature of 18°C is as shown below in figures 22,23 & 24. A 5-mW He–Ne laser beam (wavelength of 632.8 nm) is expanded and collimated. Two similar Ranchi gratings G1 and G2 of 25 lines/mm (with pitch of 0.04mm) are used to construct the Moiré fringe patterns. The distance between planes of G1 and G2 is chosen as 5mm and it is known as one of Talbot distances for the gratings used. The Talbot distances are characterized by equation (64) as $\Delta_l = l\frac{p^2}{\lambda}$, where p is the periodicity of the grating, λ is the wavelength of light and l is an integer. In this work, the Moiré fringes are formed for Talbot distance of $\Delta_{l=2} \approx 5mm$.

The diffusion cell was made of two cuvettes, 1mm thick, 90mm high and 10mm wide the longer dimension gives the direction of diffusion. The distance separating the inside surfaces was 8mm. It is placed in front of the first Grating and a 5cm convex lens placed beyond the second grating and it is followed by opal screen and digital camera respectively.

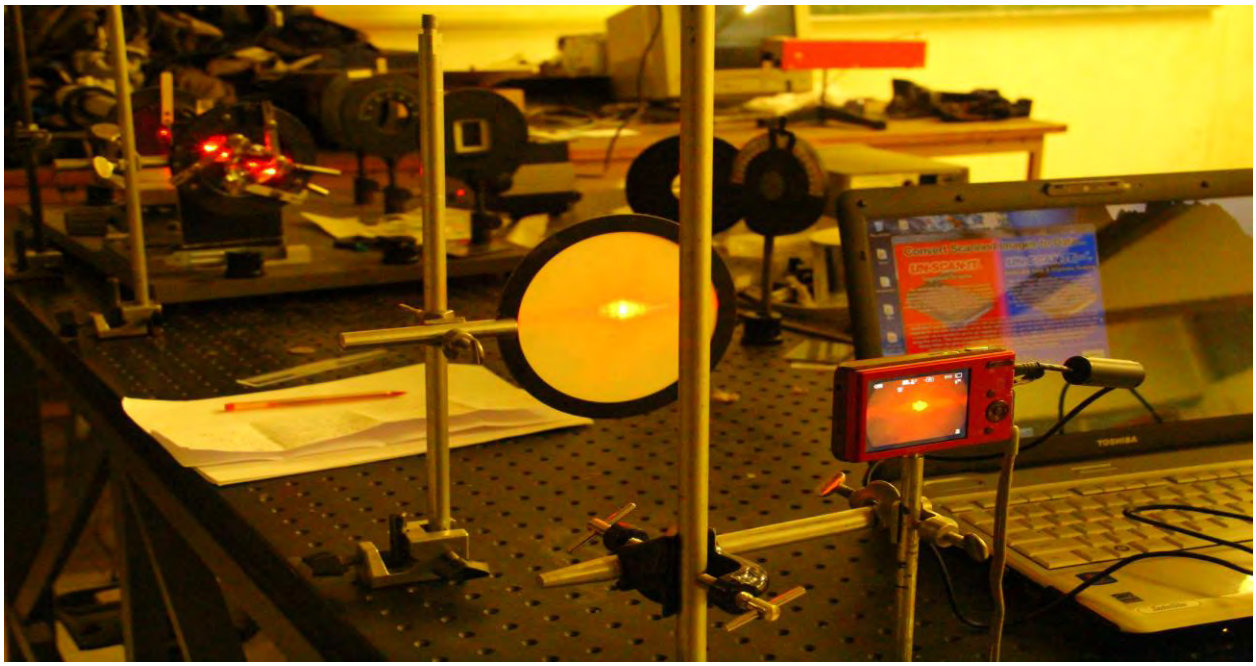

Figure 22 Experimental setup viewing from near the Digital camera.

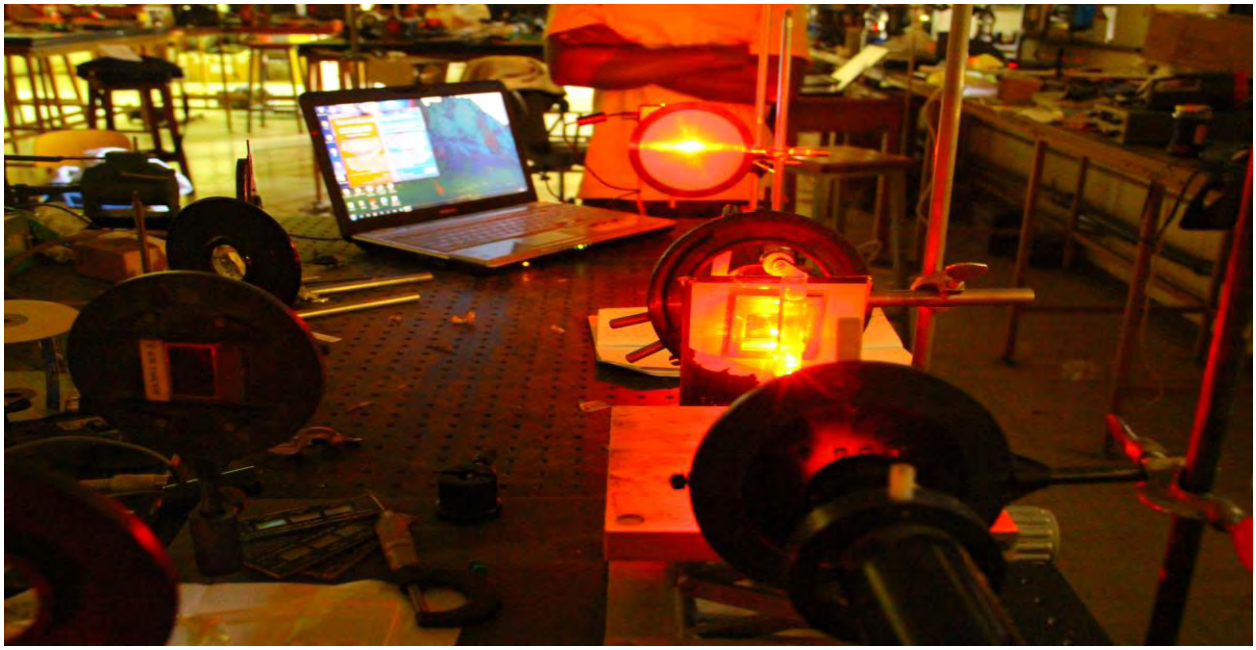

Figure 23 Experimental setup viewing near from the He-Ne laser source.

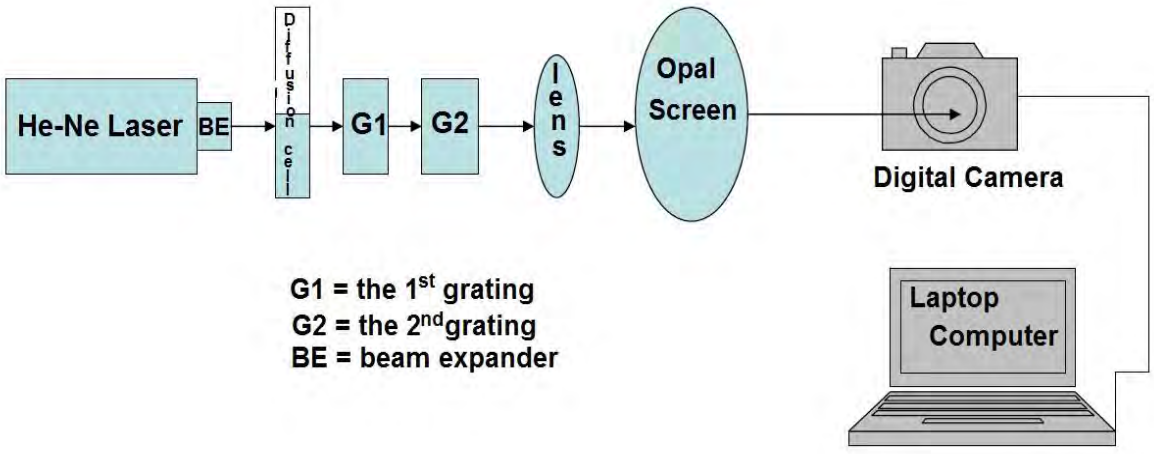

Figure 24 Diagrammatical representation of the experimental set-up.

4.3 Experimental Procedures

The cell was first half-filled with salt solution (heavier solution/higher concentration of equal volume) from below using a syringe. After allowing for residual motions to dissipate, the pure water was slowly injected on the upper part of the diffusion cell; this process took about 10 seconds. Then the He-Ne laser is released near the interface on the diffusion cell and the fringes produced by two gratings are magnified using the convex lens placed at the back of second grating. Finally the Grating patterns, during the evolution of diffusion phenomena, are captured from the opal screen at different time interval by digital camera and are stored in the computer.

CHAPTER 5

5. RESULT AND DISCUSSION

To determine the diffusion coefficient, it was necessary to transform the raw data (images) in to data sets proportional to the position of fringes and the local shift in fringes x and Δ respectively. First the software UN-SCAN-IT was used to assign (x,Δ) data points to each pixel in a single image time after time. The (x,Δ) data sets were then imported into a spreadsheet and the change in pixels for each x and Δ are converted in to millimeters(mm) and put in tables.

According to equation (83), a number of measurements of the diffusion coefficient can be made from a single Moiré pattern recorded at a desired time t_0. Therefore using equation (82) and (83) the ratio of two local shifts in fringes η and the Diffusion Coefficient D respectively for each molar solution of NaCl were calculated as below.

5.1 Results obtained for 1M NaCl solution

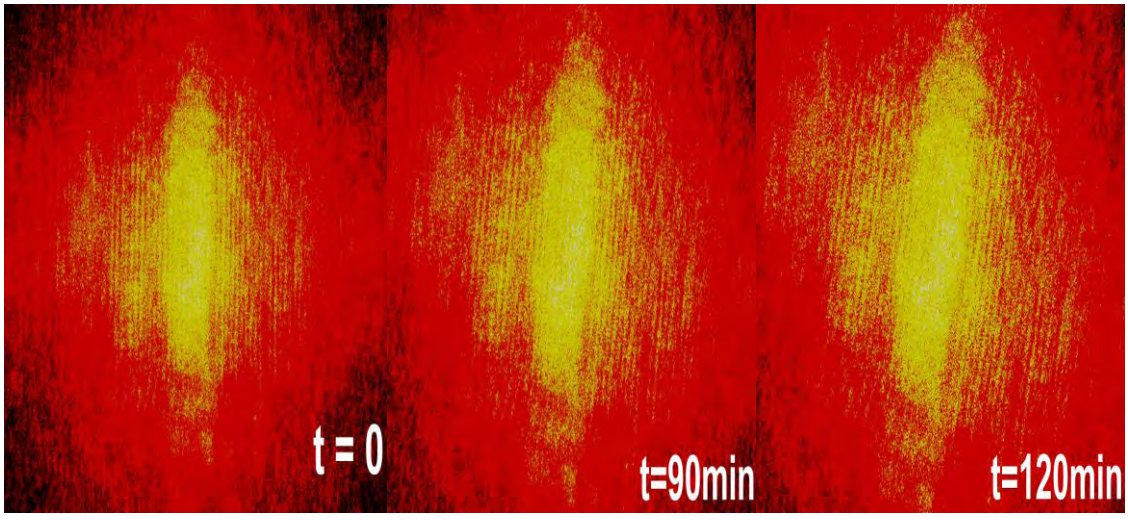

Figure 25 Moiré fringe patterns of 1M NaCl diffusion in pure water that were recorded at different diffusion times. $t_0 = 0$, $t_0 = 90\,\min$ *and* $t_0 = 120\,\min$ *. The deflectometer parameters used are:* $p = 0.04mm$, $\Delta_{l=2} \approx 5mm$ *and* $\theta = 0.03rad$.

Table 1 The position of Moiré fringes (x), the local fringe shift (Δ), the ratio of the two local shifts η and the Diffusion Coefficient D for $t_0 = 90\,\text{min}$ and $t_0 = 120\,\text{min}$

t_0	x_1	x_2	Δ_1	Δ_2	η	D
90min	2.00mm	5.00mm	2.24mm	1.20mm	1.87	$1.55\times10^{-9}\,m^2/s$
120min	3.50mm	7.00mm	3.50mm	1.50mm	2.33	$1.51\times10^{-9}\,m^2/s$

5.2 Results obtained for 2M NaCl solution

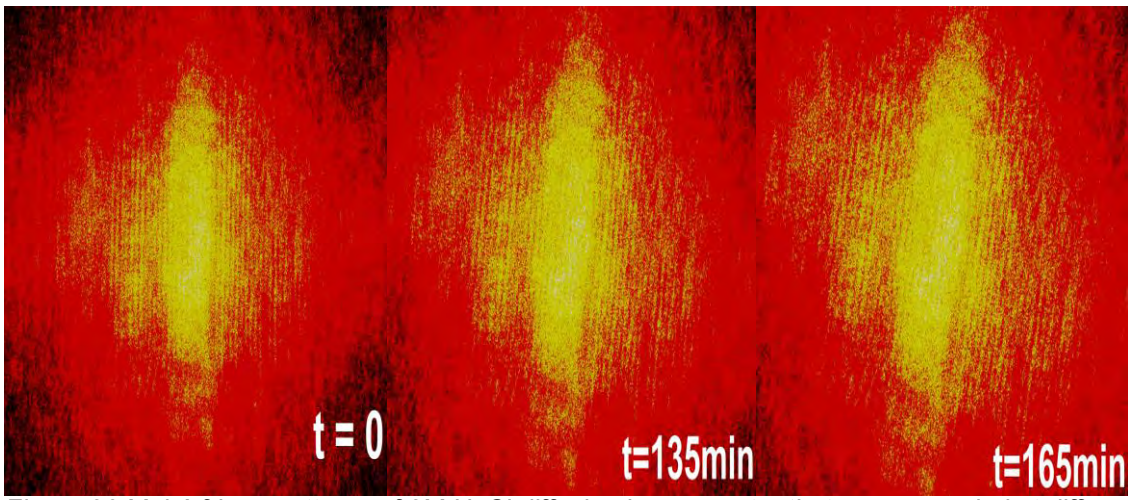

Figure 26 Moiré fringe patterns of 2M NaCl diffusion in pure water that were recorded at different diffusion times $t_0 = 0$ $t_0 = 135\,\text{min}$ *and* $t_0 = 165\,\text{min}$ *. The deflectometer parameters used are:* $p = 0.04mm$, $\Delta_{l=2} \approx 5mm$ *and* $\theta = 0.03rad$ *.*

Table 2 The position of Moiré fringes (x), the local fringe shift (Δ), the ratio of the two local shifts η and the Diffusion Coefficient D for $t_0 = 135\,\text{min}$ and $t_0 = 165\,\text{min}$

t_0	x_1	x_2	Δ_1	Δ_2	η	D
135min	5.00mm	9.00mm	5.95mm	1.99mm	2.99	$1.58\times10^{-9}\,m^2/s$
165min	7.00mm	12.00mm	9.99mm	2.25mm	4.44	$1.61\times10^{-9}\,m^2/s$

5.3 Results obtained for 3M NaCl solution

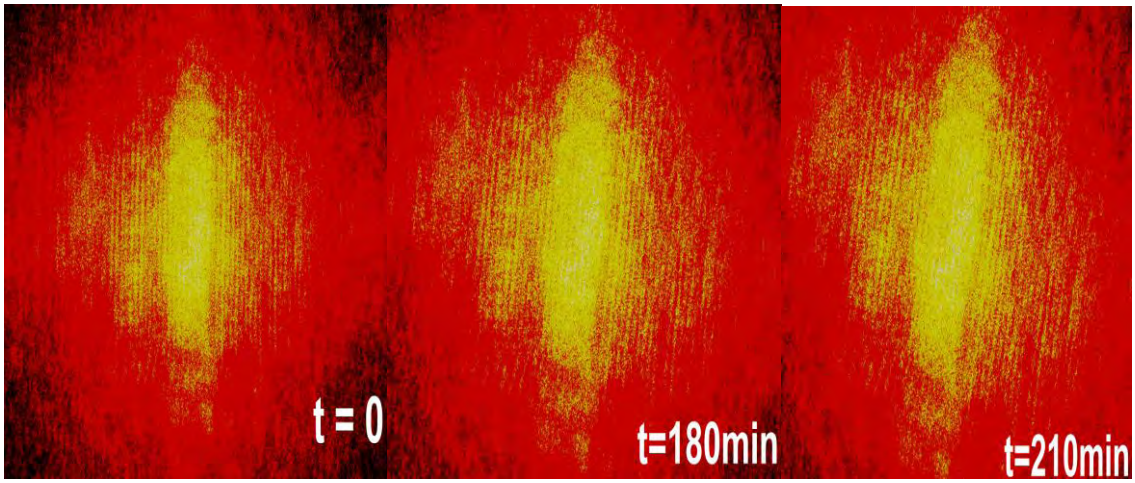

Figure 27 Moiré fringe patterns of 3M NaCl diffusion in pure water that were recorded at different diffusion times $t_0 = 0$, $t_0 = 180\,\text{min}$ *and* $t_0 = 210\,\text{min}$ *. The deflectometer parameters used are:* $p = 0.04mm$, $\Delta_{l=2} \approx 5mm$ *and* $\theta = 0.03rad$

Table 3 The position of Moiré fringes (x), the local fringe shift (Δ), the ratio of the two local shifts η and the Diffusion Coefficient D for $t_0 = 180\,\text{min}$ and $t_0 = 210\,\text{min}$

t_0	x_1	x_2	Δ_1	Δ_2	η	D
180min	10.00mm	14.50mm	14.19mm	2.75mm	5.16	$1.56\times10^{-9}\ m^2/s$
210min	13.00mm	15.00mm	10.45mm	5.00mm	2.09	$1.51\times10^{-9}\ m^2/s$

5.4 Results obtained for 4M NaCl solution

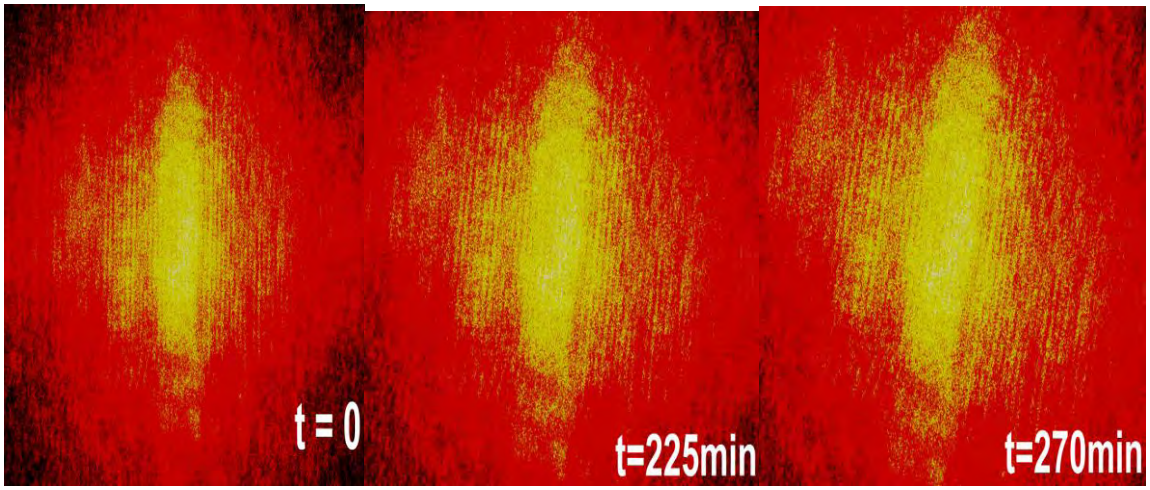

Figure 28 Moiré fringe patterns of 4M NaCl diffusion in pure water that were recorded at different diffusion times $t_0 = 0$, $t_0 = 225\,\text{min}$ *and* $t_0 = 270\,\text{min}$ *. The deflectometer parameters used are:* $p = 0.04mm$, $\Delta_{l=2} \approx 5mm$ *and* $\theta = 0.03rad$

Table 4 The position of Moiré fringes (x), the local fringe shift (Δ), the ratio of the two local shifts η and the Diffusion Coefficient D for $t_0 = 225\,\mathrm{min}$ and $t_0 = 270\,\mathrm{min}$

t_0	x_1	x_2	Δ_1	Δ_2	η	D
225min	13.00mm	16.00mm	14.43mm	5.75mm	2.51	$1.75\times10^{-9}\,m^2/s$
270min	15.00mm	17.50mm	16.52mm	7.00mm	2.36	$1.46\times10^{-9}\,m^2/s$

5.5 Results obtained for 5M NaCl solution

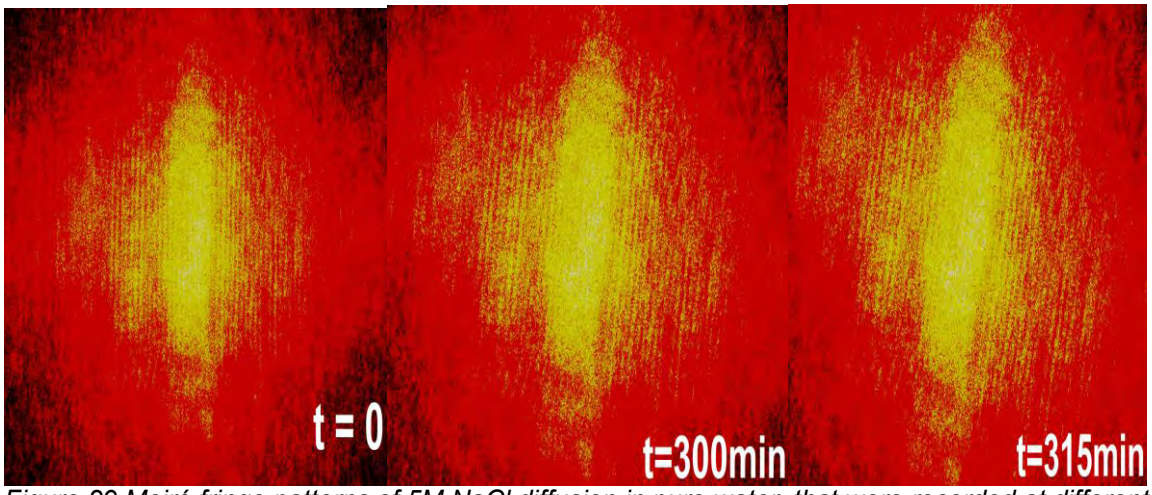

Figure 29 Moiré fringe patterns of 5M NaCl diffusion in pure water that were recorded at different diffusion times $t_0 = 0$, $t_0 = 300\,\mathrm{min}$ *and* $t_0 = 315\,\mathrm{min}$ *. The deflectometer parameters used are:* $p = 0.04mm$, $\Delta_{l=2} \approx 5mm$ *and* $\theta = 0.03rad$

Table 5 The position of Moiré fringes (x), the local fringe shift (Δ), the ratio of the two local shifts η and the Diffusion Coefficient D for $t_0 = 300\,\mathrm{min}$ and $t_0 = 315\,\mathrm{min}$

t_0	x_1	x_2	Δ_1	Δ_2	η	D
300min	16.50mm	18.00mm	12.40mm	8.00mm	1.55	$1.64\times10^{-9}\,m^2/s$
315min	18.00mm	20.00mm	17.10mm	9.00mm	1.90	$1.57\times10^{-9}\,m^2/s$

5.6 Results obtained for 6M NaCl solution

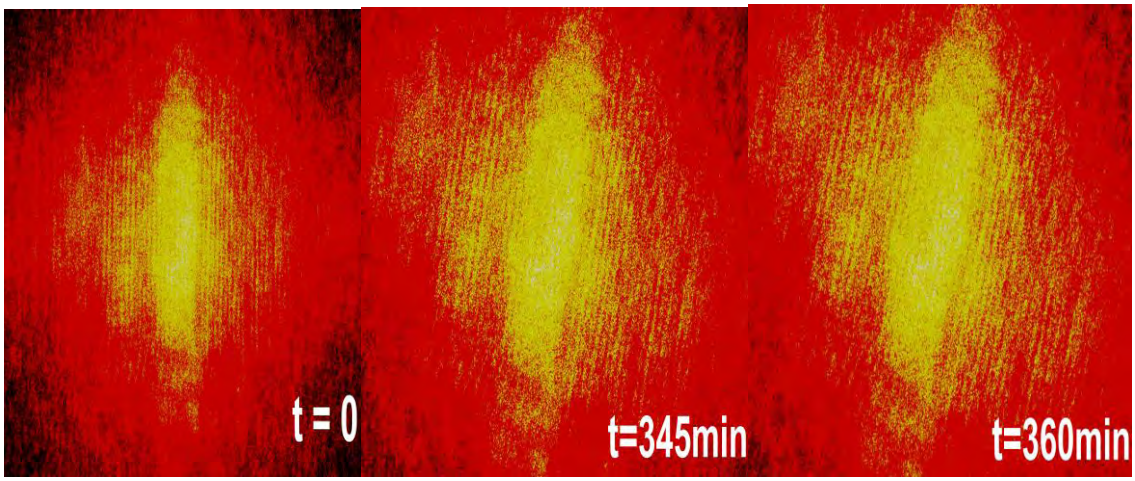

Figure 30 Moiré fringe patterns of 6M NaCl diffusion in pure water that were recorded at different diffusion times $t_0 = 0$, $t_0 = 345\,\text{min}$ *and* $t_0 = 360\,\text{min}$. *The deflectometer parameters used are:* $p = 0.04mm$, $\Delta_{l=2} \approx 5mm$ *and* $\theta = 0.03rad$

Table 6 The position of Moiré fringes (x), the local fringe shift (Δ), the ratio of the two local shifts η and the Diffusion Coefficient D for $t_0 = 345\,\text{min}$ and $t_0 = 360\,\text{min}$

t_0	x_1	x_2	Δ_1	Δ_2	η	D
345min	21.00mm	23.00mm	19.00mm	10.00mm	1.90	$1.66\times10^{-9}\,m^2/s$
360min	22.50mm	25.00mm	25.94mm	10.50mm	2.47	$1.52\times10^{-9}\,m^2/s$

In this experiment 1M NaCl as a minimum molar solution and 6M NaCl as the maximum molar solution (which is the saturation point for NaCl) were considered and it is observed that the time needed for the change in local fringe shift is different for different molar solutions but the diffusion coefficient D for the maximum as well as for the minimum solution is nearly similar.

As we can see from table (1-6) the diffusion coefficient obtained for different molar solution of NaCl in pure water using Moiré defelectometry technique is in good agreement with the diffusion coefficient obtained by other researchers using other techniques such as Interferometric measurements by Rodrigo Riquelm et al[2] they obtained $D = 1.587\times10^{-9}\,m^2/s$ and $D = 1.602\times10^{-9}\,m^2/s$ and Phase shifting interferometer by Zhixiong Guo et al[20] they obtained $D = 1.507\times10^{-9}\,m^2/s$.

CHAPTER 6

CONCULUSION AND RECOMMENDATION

6.1 Conclusion

If we take 0.03mm uncertainty in fringes shift measurements, the uncertainty in diffusion coefficient measurement would be of the order of $\pm 0.05\times 10^{-9}\, m^2/s$ therefore taking the average of the diffusion coefficients D obtained through tables 1-6 we get $D = 1.58(\pm 0.05)\times 10^{-9}\, m^2/s$ for diffusion of NaCl molecules in pure water and it is in good agreement with the reported value in literatures [2, 20]. As we have seen for different molar solutions of NaCl the Diffusion coefficient is nearly similar but the rate of diffusion varies with concentration.

6.2 Recommendation

This research was carried out on equal volume of NaCl solution and pure water at the same temperature, what happen if the volume or temperature of the system is different? This is left for other researchers.

BIBLIOGRAPHY

[1] Crank E J 1975 The Mathematics of Diffusion
(Oxford: Oxford University Press)

[2] Arun Anand, K.Vanic Chhaniwal and CS Narayana Murthy. Diffusivity Study Of Transparent Liquid solution by imaging Beam Deflection.

[3] D. Ben-Avraham and S.Havlin(2000). Diffusion and Reactions in Fractals and Disordered Systems Cambridge University Press.

[4] Weiss, G. (1994). Aspects and Applications of the Random Walk.
North- Holland.

[5] Schirripa Spagnolo, Ambrosini, and Paoletti: Liquid diffusion coefficients by digital moiré. Optical Engineering, Vol. 43 No. 4, April 2004

[6] Kazem Jamshidi-Ghaleh, Mohammad Taghi Tavassoly and Nastaran Mansour - Diffusion coefficient measurements of transparent liquid solutions using Moiré deflectometry. J. Phys. D: Appl. Phys. 37 (2004) 1993–1997

[7] Giuseppe Schirripa Spagnolo, Carla Simonetti, Lorenzo Cozzella
Measurement of mass diffusion coefficients by digital moiré.
SPIE Vol. 5958 59582Q-1

[8] N. Rashidnia, R. Balasubramaniam, J. Kuang, P. Petitjeans and T. Maxworthy. Measurement of the Diffusion Coefficient of Miscible Fluids Using Both Interferometry and Wiener's Method- International Journal of Thermophysics, Vol. 22, No. 2, 2001

[9] Rodrigo Riquelm, Ignacio Lira, Carlos Perez Lopez, Juan A. Rayas and Ramon Rodrıguez Vera. Interferometric Measurement of a Diffusion Coefficient comparison of two methods and uncertainty analysis.
J. Phys. D: Appl. Phys. 40 (2007) 2769–2776

[10] Kafri O and Glatt I 1986 Moiré deflectometry: a ray deflection approach to optical testing Opt. Eng. 24 944–60

[11] Josef Stricker - Performance of moiré deflectometry with deferred electronic heterodyne readout J. Opt. Soc. Am. A/Vol. 4, No. 9/September 1987

[12] Kung H L. Bhatnagar A. and Miller D. A B 2001 Opt. Lett. 26 1645

[13] Patroski K 1989 The self-imaging phenomenon and its applications Progress

in Optics vol. 27, ed E Wolf (Amesterdam: North-Holland) pp 1–108
[14] Born M and Wolf E 1986 Principle of Optics 6th edn (Oxford:Pergamon)
[15] Torroba R. and Tagliaferri A. A 1998 Opt. Commun. 149 213
[16] Zhixiong Guo, Shigenao Maruyama and Atsuki komiya Phy.D:Appl.Phys.32(1999)-Rapid yet accurate measurement of mass diffusion coefficients by phase shifting interferometer .
[17] Stanislaw Scieniutycz, Peter Salamon ISBN: 9780844816920 Diffusion and Rate process.
[18] Mayinger F(ed) 1994 Optical Measurments (Berlin:Springer).
[19] Bocher N and Pipman J. 1976 A Simple method of determining Diffusion Constants By Holographic Interferometery J.Phys.D:Appl.Phys.9 1825-30.
[20] Jost.W 1970 Diffusion in Solids, Liquids, Gas (New York: Acadamic)
[21] N. J. Giordano, Prentice Hall, Upper Saddle River J. (1997). Computational Physics,
[22] Eugene Hecht . Optics (4ed. AW, 2002)(ISBN 0321188780)(600dpi)
[23] Leno S. Pedrotti CORD Waco, Texas – Fundamentals of optics
[24] Moiré and Fringe Projection Techinques Optical shope Testing, second Edition, Edited by Danial Malacra. ISBN 0-471-5223-5(1992), John Wiley and Sons,inc.
[25] Josef Stricker - Performance of moiré deflectometry with deferred electronic heterodyne readout J. Opt. Soc. Am. A/Vol. 4, No. 9/September 1987
[26] M. Servin, R. Rodriguez-Vera, M. Carpio, and A. Morales - Automatic fringe detection algorithm used for moiré deflectometry
[27] Abramowitz M and Stegun I A 1972 Handbook of Mathematical Functions with Formulas, Graphs and Mathematical Tables (New York: Dover)
[28] Landau L D and Lifshitz E M 1989 Fluid Mechanics 2nd ed. (New York: Pergamon)